Study of phase transitions from short-time non-equilibrium behaviour

2011 Rep. Prog. Phys. 74 026501

(http://iopscience.iop.org/0034-4885/74/2/026501)

Rep. Prog. Phys. **74** (2011) 026501 (28pp) doi:10.1088/0034-4885/74/2/026501

Study of phase transitions from short-time non-equilibrium behaviour

E V Albano[1,2,3,5], M A Bab[1,2,3], G Baglietto[1,3,4], R A Borzi[1,2,3], T S Grigera[1,2,3], E S Loscar[1,2,3], D E Rodríguez[1,3], M L Rubio Puzzo[1,3] and G P Saracco[1,3]

[1] Instituto de Investigaciones Fisicoquímicas Teóricas y Aplicadas (INIFTA), Facultad de Ciencias Exactas, Universidad Nacional de La Plata, c.c. 16, suc. 4, 1900 La Plata, Argentina
[2] Departamento de Física, Facultad de Ciencias Exactas, Universidad Nacional de La Plata, c.c. 67, 1900 La Plata, Argentina
[3] CCT La Plata, Consejo Nacional de Investigaciones Científicas y Técnicas, Argentina
[4] Departamento de Ciencias Básicas, Facultad de Ingeniería, Universidad Nacional de La Plata

Received 18 December 2009, in final form 17 August 2010
Published 14 January 2011
Online at stacks.iop.org/RoPP/74/026501

Abstract
We review recent progress in the understanding of phase transitions and critical phenomena, obtained by means of numerical simulations of the early dynamic evolution of systems prepared at well-specified initial conditions. This field has seen exhaustive scientific research during the last decade, when the renormalization-group (RG) theoretical results obtained at the end of the 1980s were applied to the interpretation of dynamic Monte Carlo simulation results. While the original RG theory is restricted to critical phenomena under equilibrium conditions, numerical simulations have been applied to the study of far-from-equilibrium systems and irreversible phase transitions, the investigation of the behaviour of spinodal points close to first-order phase transitions and the understanding of the early-time evolution of self-organized criticality (SOC) systems when released far form the SOC regime. The present review intends to provide a comprehensive overview of recent applications in those fields, which can give the flavour of the main ideas, methods and results, and to discuss the directions for further studies. All of these numerical results pose new and interesting theoretical challenges that remain as open questions to be addressed by new research in the coming years.

(Some figures in this article are in colour only in the electronic version)

[5] Present address: IFLYSIB, C.C. 565, 1900 La Plata, Argentina.

Contents

1. Introduction

The study and the understanding of phase transitions and critical phenomena have undergone considerable progress on the basis of well-established theories such as the renormalization group and the underlying fundamental concepts of universality and scale invariance. In the neighbourhood of the critical temperature T_c of a second-order transition, the correlation length ξ grows without bounds. This single fact is the key to understanding equilibrium behaviour. Within the critical region, the universal information of a system is stored in a small set of numbers, the *critical exponents* (for example, the order parameter exponent β, the correlation length exponent ν), together with a measure of the distance to the critical point and the dimensionality of the system, d.

While most studies in the field focus on the description of equilibrium properties, a very interesting and somewhat unexpected prediction, based on a renormalization-group treatment, is that the dynamic evolution of a system at criticality—when it is released from a far-from-equilibrium initial state—is also critical. In order to achieve a qualitative understanding of this idea, let us imagine a ferromagnetic system precisely at its Curie temperature T_c, but fully saturated by an external magnetic field $\boldsymbol{B}$. The field is then suddenly turned off at an *initial time* t_0, and the system relaxes towards equilibrium. Starting from a magnetization per site $m_0 = M(t = 0)$ which is at its maximum, the spins start building up correlations while $M(t)$ slowly decreases towards zero. Due to critical slowing down, the evolution at long times of $M(t)$ is so slow that equilibrium may seem to have been reached. However, two-time functions like the spin–spin autocorrelation $A(t, s)$ (which uses a reference microstate taken at time $s \leqslant t$) show that, even in this long-time regime, the system has not equilibrated but gradually *ages*. In other words, $A(t, s)$ decreases ever more slowly when the reference configuration is taken at increasing values of s, no matter how big s and t are. Can we predict by any means the shape of $M(t)$ and $A(t, s)$ in this experiment? One might expect that the time dependence of these observables strongly depends on the microscopic interaction as well as on the dynamics chosen for the system, in addition to the details of the initial condition at time t_0. Since the critical region is dominated by non-linear phenomena, linear response theory is of no use here. However, there is a source of simplicity, which springs precisely from the complexity that appears to dominate the problem: criticality. Thanks to criticality, the final answer to the above question is not only simpler than it might seem, but it also leads to a very useful method (relatively easy to implement in numerical simulations) for studying phase transitions and measuring static and dynamic critical exponents.

The formal theory supporting these considerations was originally developed by Janssen and collaborators [1] using field-theoretic techniques. They focused on the early stages of the relaxation process after quenching the system to T_c from a very high temperature (a *critical quench*). Much more theoretical and numerical [2] work has been performed since then. Furthermore, it has been shown that the same ideas can be used in the long-time regime ($t/s \gg 1$ in the autocorrelation above) to understand and describe the critical ageing [3, 4].

The good news is that we do not need to know in detail Janssen's treatment in order understand and use the full power of the technique derived from these findings. Briefly, these results provide a way to analyse out-of-equilibrium Monte Carlo simulations of systems near criticality, from which one can obtain *equilibrium* critical exponents (including the dynamic exponent z). This is important, since it provides an alternative route to finding these exponents (without being hindered by critical slowdown or finite-size effects, see section 3.1) or, in some cases, the only possible way (see, e.g., section 3.6). The method can also be used to determine the critical temperature, or the spinodal points in the case of first-order transitions, as well as the dynamic (non-equilibrium) 'initial slip' exponent θ (defined below in section 2).

In this review, we will restrict to times when the out-of-equilibrium correlation length ξ is still very short compared either with the system size or with the equilibrium correlation length. In this context, the technique is known as *short-time critical dynamics (STCD)*. In most cases, one deals with times of the order of 10^3 Monte Carlo steps.

The aim of this paper is to provide a review and comprehensive discussion of recent work done on STCD using Monte Carlo simulations. We feel this is needed because since the early (1998) review of Zheng [2], the field has grown hugely. In particular, the method has been extended to systems not yet rigorously treated theoretically, such as non-equilibrium phase transitions, self-organized critical systems, irreversible phase transitions and spinodal points. We review these new topics together with applications to equilibrium continuous transitions.

The paper is organized as follows. Section 2 is a theoretical overview with emphasis in the key results needed to set up a Monte Carlo study of STCD. We then review applications to equilibrium (section 3) and non-equilibrium (section 4) situations. We conclude in section 5.

2. Theoretical background and method

A Monte Carlo (MC) simulation of critical short-time critical dynamics (STCD) is the analysis of the time series of a small set of observables when the control parameters (say the temperature and magnetic field) are set at their transition point values. The observables are typically the order parameter (OP) and some of its moments (called $M(t)$ and $M^{(k)}(t)$ in this section) or cumulants[6]. The analysis requires that the initial configuration be carefully controlled, sometimes fixing sharply the initial value of the order parameter (OP).

In a wide variety of Hamiltonian and dynamic systems, it turns out that the time evolution of the observables at the critical point follows a power law after an initial 'microscopic' time t_m (typically 10–100 Monte Carlo steps (MCS)) (figure 1). This is significant in itself, since it hints that this short-time approach can be used to identify the values of the critical control parameters. More important though is that the universal exponents of the transition can be directly related to the power-law exponents observed during the dynamic evolution

[6] We assume that the OP is normalized so that its maximum possible value is 1.

of the aforementioned observables. Obtaining the universal exponents together with the critical control parameters is one of the main goals of the technique.

The theoretical description of the critical STCD for Hamiltonian systems with dissipative Langevin dynamics (model A in the classification of Hohenberg and Halperin [5]) was originally provided by Janssen *et al* [1]. This aspect has already been quite comprehensively reviewed, in the context of ageing of critical systems, by Calabrese and Gambassi [3]. The latter authors have recently extended the theory (which was originally restricted to the evolution of an initially disordered state, $m_0 \approx 0$) to encompass partially ordered initial states [6]. They use the same type of dynamics as in [1] on the ferromagnetic Ising [6] and vector models [7]. Here we will not focus on the foundations, but mainly on those theoretical facts and methods that concern the application of the technique to extract information about the phase transition using computer simulations.

A typical STCD computer experiment starting from a disordered configuration may be described as follows. The initial microstate is chosen such that the system is mostly disordered ($m_0 \ll 1$) and with negligible spatial correlations. Then the system is allowed to evolve for a time that is short with respect to the time required for equilibration. This protocol is repeated many times in order to obtain a time series averaged over the thermal histories and initial conditions.

In general, the outcome of the experiment will depend on m_0, on the control parameters (collectively represented here by the adimensional ratio $\tau = (T - T_c)/T_c$) and on the linear size L of the system. To describe the time evolution of the moments, we assume the following scaling ansatz for the kth moment of the OP [1, 2],

$$M^{(k)}(t) \equiv \langle M^k(t) \rangle \sim b^{-k\beta/\nu} M^{(k)}(b^{-z}t, b^{1/\nu}\tau, L/b, b^{x_0}m_0), \tag{2.1}$$

where $\langle \ldots \rangle$ means average over runs with identical initial value of the OP but different initial configurations and realizations of the dynamics; b is a rescaling spatial parameter; β, ν and z are the usual critical exponents (see, e.g., [8]) related to the growth of OP, correlation length ξ and correlation time, respectively and x_0 is a new exponent which describes the dependence of the moments on m_0 during the short-time regime. The first two critical exponents are not affected by details such as the particular choice of the lattice geometry or the dynamic rules employed, but the value of z will strongly depend on the features of these rules.

In order to point out the main goals of the short-time procedure, we will briefly develop some examples of how the scaling laws are obtained from (2.1), and from them, how the values of the control paremeters and critical exponents can be estimated.

Suppose that a MC simulation is started as described above, very near the critical point. Since the spatial correlations are negligible, the system behaves initially mean-field-like, and after a given time $t > t_m$, $M(t)$ initially *grows* [9] (figure 1(*a*)). Once correlations become important, $M(t)$ decreases to its equilibrium value. Thus, there must be a crossover between this initial increase and the long-time decrease, as exemplified in figure 1(*a*) (inset). We can extract

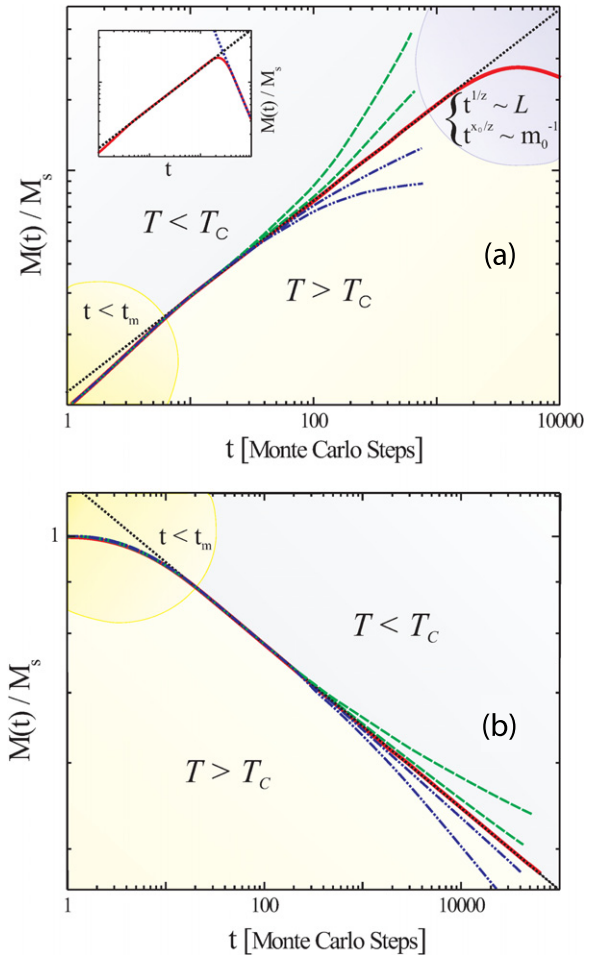

Figure 1. Scheme for short-time dynamics experiments taking as an example the evolution of the order parameter from an almost disordered (*a*) or totally ordered initial state (*b*). (*a*): starting from a fixed initial value m_0, the normalized average OP $M(t)/M_s$ (M_s is the saturation value) is shown as a function of time in a log–log plot. The time values given are representative of the actual MC times used in practice, while the y-scale is left unspecified as it strongly depends on the system and observable chosen (values for the initial slip exponent θ would only be accurate in the limit $m_0 \to 0$). After a microscopic time t_m, the critical curves follow a power-law behaviour. If the correlation length $\xi(t)$ grows to become similar to the equilibrium correlation length $\xi_{eq}(T)$, the curves cross over to an exponential decay towards the equilibrium value of M (dashed and double-dot-dashed curves). At the critical point, specified by T_C (full-line curve), the system will eventually cross over to the long-time regime critical decrease (see inset), or will decay exponentially when $\xi(t) \approx L$. (*b*): when starting from an ordered state, we expect a single power law at the critical point that extends even to the long-time regime. When finite-size effects can be neglected, this fact makes the fully ordered initial condition better suited to accurately determine the critical control parameters.

this behaviour from (2.1) by imposing, after Janssen *et al* [9], certain conditions on the functional form of $M^{(1)}$. By assuming that the time-dependent correlation length $\xi(t) \sim t^{1/z}$ is small compared with both the lattice size L and the equilibrium correlation length $\xi_{eq}(T) \sim \tau^{-\nu}$, and setting $b = t^{1/z}$, equation (2.1) can be rewritten as

$$M(t) \sim t^{-\beta/\nu z} M^{(1)}(1, t^{1/\nu z}\tau, L/t^{1/z}, t^{x_0/z}m_0)$$
$$= t^{-\beta/\nu z} F(t^{x_0/z}m_0), \tag{2.2}$$

which is expected to be valid within the time regime $L/t^{1/z} \gg 1$ and $\xi_{eq}(T)/t^{1/z} \gg 1$. Also, $F(x)$ must satisfy $F(x) \sim x$ for $x \ll 1$ and $F(x) \sim$ constant for $x \gg 1$ [9]. In this way, we obtain the initial OP increase,

$$M(t) \sim t^{x_0/z-\beta/\nu z} \sim t^{\theta}, \qquad m_0 t^{x_0/z} \ll 1, \tag{2.3}$$

which defines the 'initial slip' exponent θ. This increase in $M(t)$ is expected at the critical point (and somewhat above it as long as $t_m^{1/z} \ll \xi(T)$), and provided that the system is below the upper critical dimension (for a mean-field model, we expect $\theta = 0$ [1]). On the other hand, for longer times we get the usual critical decrease,

$$M(t) \sim t^{-\beta/\nu z}, \qquad m_0 t^{x_0/z} \gg 1. \tag{2.4}$$

The crossover time can be determined from the relation $m_0 t^{x_0/z} \sim 1$. Note that, in order to observe an initial increase in $M(t)$, a small but non-zero value for m_0 is needed, because usually OPs are antisymmetric under reflections of m_0 (i.e. $M(t, m_0) = -M(t, -m_0)$, implying that $M(t, m_0 = 0) = 0$ for all t. Furthermore, if one of the above assumed conditions is unfulfilled, the power law will be modulated by the scaling function $M^{(1)}$. This happens when $\xi(t) \sim L$ or $m_0 t^{x_0/z} \approx 1$ (full curve in figure 1(*a*)), or when τ is not set at the critical value (dashed and double-dot-dashed curves in the same figure). If this is the case, there will be a time $t_l(\tau) \sim \tau^{-\nu z}$ at which the correlation length approaches its equilibrium value. For $t > t_l(\tau)$, the power law will cross over to an exponential relaxation towards the equilibrium value of the OP (dashed and double-dot-dashed curves in figure 1). This seeming difficulty can be turned over into an advantage, since it can be used to determine the value of the critical control parameter [2]. Modern computers are usually powerful enough to run simulations in systems where size effects can be neglected, so that the crossover to the late time regime tends to be the main interference with the predicted power-law behaviour at $\tau = 0$. As will be mentioned below, this crossover is not present when we start from a fully ordered initial state (figure 1(*b*)), making this second possibility better suited to determine the critical parameters. The sensitivity of $M(t, \tau)$ to τ can be such as to allow the determination of the critical point with high precision (≈1% is a typical value).

So far we have referred to initial conditions in which m_0 is sharply defined. This restriction can be relaxed to have m_0 determined by a probability distribution. However, it is important to stress that departures from a sharp preparation of the initial macrostate could have an effect on the performance of the procedure, depending on the sensitivity of the particular system to the value of m_0.

Another observable that displays a power law at short times is the fluctuation of the OP,

$$\Delta M^{(2)}(t) \equiv \langle M^2(t)\rangle - \langle M(t)\rangle^2 = M^{(2)}(t) - [M^{(1)}(t)]^2. \tag{2.5}$$

As long as $\xi(t) \ll L$, the fluctuations will behave as $\sim L^{-d}$ according to the central limit theorem. Since $\Delta M^{(2)}(t) > 0$ and the initial conditions force $\Delta M^{(2)}(0) = 0$, we expect a steady increase with time even for $m_0 = 0$. Setting $b = t^{1/z}$, $\tau = 0$ in (2.1), assuming $t^{x_0/z} m_0 \ll 1$ and imposing $\Delta M^{(2)} \sim L^{-d}$ one obtains

$$\Delta M^{(2)} \sim t^{-2\beta/\nu z} \times (L t^{-1/z})^{-d} = L^{-d} t^{(d-2\beta/\nu)/z}, \tag{2.6}$$

plus corrections of order $t^{x_0/z} m_0$. This can also be written

$$\Delta M^{(2)} \sim t^{\gamma/\nu z} \tag{2.7}$$

if the hyperscaling relation $d\nu - 2\beta = \gamma$ holds.

Proceeding in a similar way, one can investigate the critical time behaviour of other moments, their derivatives or combinations of them. In general, it is necessary to measure several of those quantities to extract the (thermodynamic) critical exponents. Some particularly useful cases are summarized in table 1 for future reference.

The spin–spin time autocorrelation function $A(t) \equiv A(t, s = 0)$ deserves special attention. For a magnetic system in a lattice of N sites, it is defined as

$$A(t) \equiv \frac{1}{N} \sum_{i=1}^{N} \langle s_i(0) s_i(t)\rangle, \tag{2.8}$$

where $s_i(t)$ is the value of spin i. At the critical point and when starting from a random initial configuration (critical quench), describing the decay of this function requires a *new* critical exponent. This fact was first noticed by Huse [10] in a MC study, and the scaling form $A(t) \sim t^{\theta - d/z} \equiv t^{-\lambda}$ was first derived Janssen *et al* [1]. The need for a new exponent for this function is related to very the existence of the initial slip exponent θ. While it might seem paradoxical to find a dependence on θ for a critical evolution from an initial condition in which m_0 is forced to be zero, this corresponds to the fact that x_0 is not only the scaling dimension for the macroscopic initial magnetization, but is also related to its density value [2].

Finally, it is natural to ask what the effect of choosing an initial state different from (near) full disorder will be. We shall only consider the case of a completely ordered state. Given that in this case $m_0 = 1$, the time dependence of the moments $M^{(k)}(t)$ is

$$M^{(k)}(t) \equiv \langle M^k(t)\rangle = b^{-k\beta/\nu} M^{(k)}(b^{-z} t, b^{1/\nu}\tau, L/b), \tag{2.9}$$

where the dependence on m_0 has been dropped because it is an irrelevant operator for this second trivial fixed point [2, 6]. This second condition allows the extraction of more information from the system, which can be used either to complete or to cross-check the results obtained when departing from disorder.

It is relatively easy to write down the corresponding critical scaling laws, proceeding as shown above. In this case, these laws should hold even in the long-time regime (for an infinite system tuned at $\tau = 0$). The scaling for some useful quantities in the ordered initial condition case is also given in table 1.

3. Equilibrium phase transitions

As discussed in section 2, the theory of STCD was developed originally for the case of the critical point of (equilibrium)

Table 1. Summary of the most-used scaling relations valid for critical dynamics. $M(t)$ and $M^{(k)}(t)$ stand for the order parameter and its kth moment, respectively. We also include the fluctuation of the order parameter, $\Delta M(t) = \langle M^{(2)}\rangle - \langle M\rangle^2$, the second-order Binder cumulant $U(t)^{(2)} = \frac{\langle M^{(2)}\rangle}{\langle M\rangle^2} - 1$, the fourth-order Binder cumulant $U(t)^{(4)} = 1 - \frac{\langle M^{(4)}\rangle}{3\langle M^{(2)}\rangle^2}$, the logarithmic derivative $\partial_\tau \log M(t,\tau)\,|_{\tau=0}$ of the order parameter and the autocorrelation $Q(t) = \langle M(t)M(0)\rangle$. Other correlations can be studied in this fashion; for example, in spin systems it is useful to consider the spin–spin autocorrelation, $A(t) = \langle \frac{1}{N}\sum_i^N s_i(t)s_i(0)\rangle$.

Initial state	Scaling relations
Ordered	
$m_0 \equiv 1$	$M(t)^{(k)} \sim t^{-k(\beta/\nu z)}$
	$\Delta M(t) \sim t^{(d/z-2\beta/\nu z)}$
	$U(t)^{(2)} \sim t^{d/z}$
	$\partial_\tau \log M(t,\tau)\,|_{\tau=0} \sim t^{1/\nu z}$
Disordered	
$m_0 \to 0$	$M(t) \sim t^{(x_0/\nu z-\beta/\nu z)=\theta}$
$m_0 \equiv 0$	$\Delta M(t) \sim t^{(d/z-2\beta/\nu z)}$
	$U(t)^{(4)} \sim t^{\frac{d}{z}}$
	$\partial_\tau \log M(t,\tau)\,|_{\tau=0} \sim t^{1/\nu z}$
	$A(t) \sim t^{(\theta-d/z)}$
$\langle m_0\rangle = 0$	$Q(t) \sim t^{\theta}$

second-order phase transitions. Hence a very large number of numerical studies have been carried out in such a case; we review the most recent results in the section 3.1, referring to [2] for earlier work. STCD has also been studied for Kosterlitz–Thouless transitions (section 3.2), spin glasses (section 3.3), the helix–coil transition (section 3.4) and damage spreading (section 3.5). At a first-order transition point, there is typically no critical behaviour; however, STCD is relevant in the study of the points (surrounding the transition point) where the phases become unstable, i.e. the (pseudo)spinodals. This we discuss in section 3.6.

3.1. Second-order transitions

Here we start by discussing critical dynamics at second-order transitions of short-range (section 3.1.1) and long-range (section 3.1.2) spin models. We next consider multicritical points (section 3.1.3), where the critical dynamics is different from ordinary second-order transitions. Universality can also be affected by topological effects (section 3.1.4) and disorder (section 3.1.5). Real systems are bounded by surfaces or contain defects. Surfaces can alter universal behaviour or cause non-universal criticality. These we discuss in section 3.1.6. Finally, in section 3.1.7 we consider defects and other cases leading to non-universal behaviour.

3.1.1. Short-ranged spin models. The STCD approach has been applied to the study of second-order phase transitions in several short-ranged models by means of MC simulations [2, 11–19]. In this section, we review recent results obtained from the dynamic evolution of the physical observables at criticality, after the system was annealed from its ground (ordered) state and quenched from its high-temperature uncorrelated (disordered) state. Results from before 1998 have been reviewed in [2].

Ising and Potts are the models which have been most extensively studied (including the corrections that arise from topological and disorder effects; see sections 3.1.4 and 3.1.5). The degrees of freedom of the q-state Potts model are spins S_i taking integer values in the range $1, \ldots, q$. The Hamiltonian is

$$H = -J \sum_{\langle i,j\rangle} \delta_{S_i S_j}, \tag{3.1}$$

where $\delta_{S_i S_j}$ is the Kronecker delta. In the short-range version, spins are placed in some lattice, and the sum is over nearest neighbours (NNs), which we denote with $\langle i, j\rangle$. $J(>0)$ is the exchange coupling constant (we have chosen the sign for the ferromagnetic version). When $q = 2$, we can choose $S_i = \pm 1$, so that $\delta_{S_i S_j} = (1 + S_i S_j)/2$; this case is thus equivalent to the Ising model. In two dimensions, the Potts model has been solved exactly for all q [20]. It has a second-order phase transition for $q \leqslant 4$ and a first-order one for $q > 4$. The critical temperature is $k_B T_c = \frac{J}{\ln(1+\sqrt{q})}$ [20].

For an STCD study, the order parameter (OP) is defined as

$$M(t) = \frac{q}{(q-1)L^d}\left\langle \sum_i \delta_{S_i S_j} - \frac{1}{q}\right\rangle. \tag{3.2}$$

Note that for $q = 2$, the usual Ising OP is recovered. Table 2 summarizes the critical exponents as obtained from STCD scaling (i.e. by employing the expressions given in table 1) as well as the exact values, when known. This table also includes the SU(2) lattice gauge theory [21] and the quantum transverse Ising model [22] that are in the same universality class as the 2D Ising model as far as static behaviour is concerned [23–25]. In order to investigate whether universal scaling behaviour also exists in deterministic dynamics, the 2D ϕ^4 theory was studied by taking the average kinetic energy as the control parameter and the magnetization as the OP [26]. In this case, the STCD scaling forms were assumed for processes starting from a random state, and the obtained critical exponents are also shown in table 2.

The STCD has also been studied for three-spin models. Interactions involving an odd number of spins have been found to be important in the description of some magnetic systems [31] or to model lattice gases with multiple-body interactions. Two such models are the 2D Ising with three-spin interactions in one direction (IMTSI) [32] and the Baxter–Wu (BW) model [33, 34]. These models show a second-order phase transition but are not invariant by a global inversion of all spins. The respective Hamiltonians are

$$H = -J \sum_{i,j} \{S_{i,j}\, S_{i+1,j} S_{i+2,j} + S_{i,j} S_{i,j+1}\} \qquad \text{(IMTSI)} \tag{3.3}$$

and

$$H = -J \sum_{\langle i,j,k\rangle} S_i S_j S_k \qquad \text{(BW)}, \tag{3.4}$$

where in IMTSI the sum is over all sites of a square lattice and $S_{i,j}$ is the spin variable placed at the site (i, j). In the BW model, the S_i are located at the sites of a triangular lattice, and the sum is over all elementary triangles. Both Hamiltonians are invariant under reversal of all the spins belonging to two of the three sub-lattices into which the original lattice can be

Table 2. Static ($2\beta/\nu$, β and $1/\nu$) and dynamic (z and θ) exponents obtained from a short-time critical dynamics (STCD) analysis for several models, together with exact values when known. (*) Indicates numerical estimation.

Model	$2\beta/\nu$	β	$1/\nu$	z	θ
2D Ising	0.252(2) [2]	0.124(5) [2]	1.02(4) [2]	2.166(7) [27]	0.191(1) [28]
(exact)	1/4	1/8	1	2.1667(5)* [29]	—
3D Ising	0.517(2) [13]	0.3273(17) [13]	0.6327(20) [13]	2.042(6) [13]	0.108(2) [13]
2D Potts $q = 3$	0.2660(6) [11]	0.107(3) [11]	1.24(3) [11]	2.196(8) [11]	0.075(3) [28]
(exact)	4/15 [20]	1/9 [20]	6/5 [20]	—	—
2D Potts $q = 4$	0.248(3) [12]	0.0830(6) [12]	1.495(13) [12]	2.290(3) [30]	−0.046(9) [12]
(exact)	1/4 [20]	1/12 [20]	3/2 [20]	—	—
SU(2)	0.240(36) [21]	—	—	2.135(27) [21]	0.192(2) [28]
Transverse Ising	0.23(5) [22]	0.119(2) [22]	0.97(1) [22]	1.883(7) [22]	
2D ϕ^4	0.24(3) [26]	0.11(7) [26]	1.05(6) [26]	2.148(20) [26]	0.176(7) [26]

Table 3. Critical exponents obtained from STCD for the 2D Ising model with three-spin interactions in one direction (IMTSI), the Baxter–Wu (BW) model, m and the 2D $q = 4$ Potts model, which belongs to the same universality class. The values of the exponents θ and z have been the subject of some controversy (see text).

Model	β	$1/\nu$	z	θ
IMTSI [35]	0.11(2)	1.487(12)	2.380(4)	−0.03(1)
BW [18]	0.079(2)	1.54(2)	2.294(6)	−0.185(1)
2D Potts $q = 4$ [12]	0.0830(6)	1.495(13)	2.290(3)	−0.046(9)

decomposed, i.e. they exhibit semi-global up–down reversal symmetry. The OP of both models is the usual magnetization ($M = \frac{1}{L^d}\sum_i S_i$), and their ground state is fourfold degenerate: three of these states have magnetization equal to $-1/3$, while the remaining state has a magnetization equal to 1. Santos and Figueiredo [15] have shown for the BW model that the initial ground state is irrelevant for the relations involved in the relaxation dynamics. Table 3 summarizes the values of the exponents obtained through STCD. Based on the value of the exponent ν and on the symmetry of the Hamiltonian, several researchers have included these models in the universality class of the 2D four-state Potts model [18, 34–36].

Although the static critical behaviour of these models is well understood, there are still controversies about the dynamic behaviour. For instance, for the BW model, Santos and Figueiredo [15] have found $z = 2.07(1)$ for the dynamic evolution from the ground state with $m_0 = 1$ (all sub-lattices initially with spins up), and $z = 1.96(2)$ for the evolution from the ground state with $m_0 = -1/3$ (spins are initially up in one sub-lattice and down in the other two). However, Arashiro *et al* [18] have obtained a value of $z = 2.294(6)$, which is close to values obtained for the IMTSI model [35] and for the 2D four-state Potts models [30] (see table 3). Moreover, the estimated exponent $\theta = -0.185(1)$ for the BW model [18] is completely different from the values computed for the IMTSI [35] and 2D four-state Potts models [12] (table 3). More recently, Arashiro *et al* [37] compared the STCD of the $q = 4$ Potts and BW models (in 2D) in extensive MC simulations which also measured the global persistence probability $P(t)$ that the order parameters have not changed sign up to time t (this quantity is known to decay at the critical temperature as $P(t) \sim t^{\theta_g}$ [38]). The dynamic exponent θ_g was obtained, finding a clear difference between the Potts and BW models. The usual dynamic critical exponents θ, z, x_0 were obtained with more precision but in good agreement with previous results [12, 35].

The STCD of the Heisenberg model has been studied by Fernandes *et al* [19]. The classical Heinsenberg model is defined by

$$H = -J \sum_{\langle i,j \rangle} \boldsymbol{S}_i \cdot \boldsymbol{S}_j, \tag{3.5}$$

where $\boldsymbol{S}_i$ is a 3D vector of unit magnitude located at each lattice site, and the sum runs over all nearest neighbours. This model has a 3D OP and it undergoes a second-order phase transition at $T_c = \frac{J}{k_B}1.44292(8)$ [39] for $d = 3$. Fernandes *et al* [19] applied STCD scaling to one Cartesian component of the magnetization (OP). The computed static exponents β and $1/\nu$, and the dynamic exponent z obtained by STCD method (see table 4), were in good agreement with the values found by equilibrium MC [39]. Zelli *et al* studied the STCD of the Heisenberg model on a 3D stacked triangular lattice with antiferromagnetic interaction on the layers and ferromagnetic interactions between layers [40]. These authors provided strong evidence for the existence of a weak first-order phase transition in this case [40].

STCD was also studied for the classical spin model with double-exchange interaction (DE) [41]. The DE model has played an important role in the study of colossal magnetoresistence, i.e. the extremely large (many orders of magnitude) change in resistivity upon application of magnetic field observed in some Mn-based perovskite oxides known as manganites. The Hamiltonian is

$$H = -J \sum_{\langle i,j \rangle} \sqrt{1 + S_i S_j}, \tag{3.6}$$

where the S_i are 3D vectors of unit magnitude as in the Heisenberg model. The critical temperature is $T_c = \frac{J}{k_B}0.74515$ [42]. Fernandes *et al* [41] determined the critical exponents, which are shown in table 4. They are in good agreement with previous estimates [42] and support the assertion that the classical DE model belongs to the universality class of the classical Heisenberg model.

Finally, let us mention that Környei *et al* [43] have studied the effects of a sudden variation in the form of the interaction, i.e. a 'quench', where instead of the temperature, the coupling constants are altered so as to suddenly change the universality class. The authors considered (in 2D) interactions of the Ising,

Table 4. Critical exponents obtained by means of the STD scaling analysis for the 3D classical Heisenberg model and classical double-exchange interaction model (DE), which belong to the same universality class.

Model	β	$1/\nu$	z	θ
3D-Classical Heisenberg [19]	0.361(2)	1.456(13)	1.976(9)	0.482(3)
3D-Classical DE [41]	0.356(6)	1.458(21)	1.975(10)	0.480(7)

IMTSI and BW kind. For an initial configuration at the critical point, the relaxation of the magnetization and the decay of the autocorrelation function were studied. They were found to display a power-law behaviour, with exponents depending on the universality class of the initial interactions.

3.1.2. Long-ranged spin models. The critical behaviour of systems with long-range interactions is still a challenging topic in statistical physics [44–46]. In particular, the dynamic evolution of these systems when starting far from equilibrium poses difficulties because the relevant observables relax rather fast due to the long-range interactions. For these reasons, the study of STCD in simple long-range models such as Ising and Potts plays an important role in the understanding of the dynamics of second-order phase transitions. The STCD scaling has been extended to the case of interactions decaying with a power law for the continuous n-vector model [44], the random Ising model [47] and the kinetic spherical model [48, 49]. However, only a few numerical results have been reported, for the 1D Ising and Potts models [50, 51]. The Hamiltonian is

$$H = -\sum_{i>j} \frac{J}{r_{i\neq j}^{1+\sigma}} \delta_{S_i S_j}, \tag{3.7}$$

where $J > 0$ is the (ferromagnetic) coupling constant, $S_i = 1, \ldots, q$ is the spin variable at site i, $r_{i,j} = |r_i - r_j|$ is the distance between spins and the sum is over all pairs of spins. The decay of the interaction strength is controlled by the parameter σ. It is well known [52] that for $0 < \sigma < 1$, the model has a second-order phase transition for all q. For $q = 2$ (Ising model), the critical behaviour is mean-field for $0 < \sigma \leqslant 0.5$, while for $0.5 < \sigma < 1$, the critical exponents are σ-dependent. For $q = 3$, the σ-dependent range is $\sigma_c(q = 3) < \sigma < 1$, with $\sigma_c(3) = 0.72(1)$. For $\sigma < \sigma_c(q = 3)$, the transition is first order [53]. For both $q = 2$ and $q = 3$, short-range behaviour is observed for $\sigma > 1$, while a Kosterlitz–Thouless transition has been predicted for $\sigma = 1$ [53, 54]. The dynamic exponents z and θ determined through the STCD evolution from the uncorrelated initial state are shown in table 5, together with RG predictions. The discrepancies between the numerical and RG results have been attributed to shortcomings of the ϵ-expansion, possibly indicating the need to go beyond two loops [44, 50].

For $\sigma = 0.75$, static exponents were also obtained from STCD behaviour, $\gamma/\nu = 0.748(11)$, $\beta/\nu = 0.126(5)$ and $\nu = 0.47(2)$ [51], which are in good agreement with RG predictions $\gamma/\nu = \sigma = 0.75$, $\beta/\nu = \frac{1-\sigma}{2} = 0.125$ and $\nu = 0.4765$ [44, 55, 56].

Table 5. Dynamical critical exponents (θ and z) of the 1D Ising and 1D $q = 3$ Potts models, as obtained by STCD scaling for the different values of the interaction control parameter σ. Also quoted are RG results [44]. The discrepancies are thought to be shortcomings of the ϵ-expansion in the latter approach.

Model	σ	θ	z	θ_{RG}	z_{RG}
1D Ising [50]	0.90	0.212(5)	1.18(4)	0.3346	0.9532
1D Ising [50]	0.80	0.188(4)	0.96(4)	0.2587	0.8340
1D Ising [51]	0.75	0.211(7)	0.868(9)	0.2171	0.775
1D Ising [50]	0.70	0.137(6)	0.81(1)	0.1733	0.7174
1D Ising [50]	0.60	0.07(1)	0.70(1)	0.0821	0.6052
1D Potts $q = 3$ [50]	0.90	0.120(4)	0.121(1)	—	—
1D Potts $q = 3$ [50]	0.80	0.058(4)	0.101(4)	—	—

3.1.3. Multicritical behaviour. Points that lie in the border of a critical manifold or at the intersection of two or more critical manifolds are called *multicritical,* and normally belong to a universality class different from that of the neighbouring critical points [57]. Multicritical phenomena have been the subject of intense study for more than half a century, both experimentally and theoretically. One of the first multicritical systems investigated is the Blume–Capel (BC) spin-1 model [58], which has been used to describe the behaviour of ^{3}He–^{4}He mixtures [57]. Apart from its experimental relevance, the model is of intrinsic interest since it is the simplest generalization of the Ising model that exhibits a rich phase diagram. The Hamiltonian is

$$H = -J \sum_{\langle i,j \rangle} S_i S_j + D \sum_i S_i^2 + h \sum_i S_i, \tag{3.8}$$

where $S_i = 0, \pm 1$, and the sum runs over all NN. D corresponds to the crystal field anisotropy, J is the exchange coupling constant and h is an external field.

The BC has a *tricritical* point, where three critical lines intersect. At zero external field, the ordered (ferromagnetic, $F_\pm$) and disordered (paramagnetic, F_0) phases are separated by a line of transitions that change from second order to first order at the tricritical point (see figures 2 and 3). Along the critical (λ) line, the behaviour is Ising-like, with exponents that reach the values of the Ising model in the limit $D \to -\infty$ [59, 60]. The behaviour changes at the tricritical point, where it is more complex, for instance the exponent θ is expected to become negative [61]. The tricritical point was determined using conformal invariance and finite-size scaling as $k_B T_t/J = 0.609(4)$ and $D_t/J = 1.965(5)$ [62]. The tricritical exponents β and $1/\nu$ were determined by conformal invariance as $\beta = 1/24$ and $1/\nu = 9/5$ [63]. STCD was used to estimate the exponents [59]; it was also found that z and θ become more Ising-like as D becomes more negative (see table 6).

Tricritical points also occur in some metamagnetic systems [65] with competing ferro- and antiferromagnetic interactions (metamagnets are systems which undergo a first-order transition with a magnetization jump at a finite magnetic field). A simple 2D model of a metamagnet can be obtained by placing spins in a square lattice formed by two alternating sub-lattices such that the coupling between spins of the same

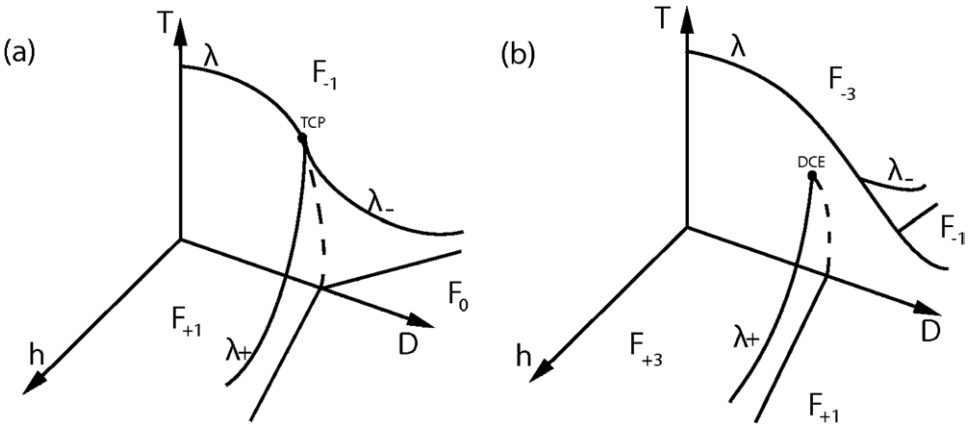

Figure 2. Schematic phase diagram of the Blume–Capel spin-1 (*a*) and spin-3/2 (*b*) models.

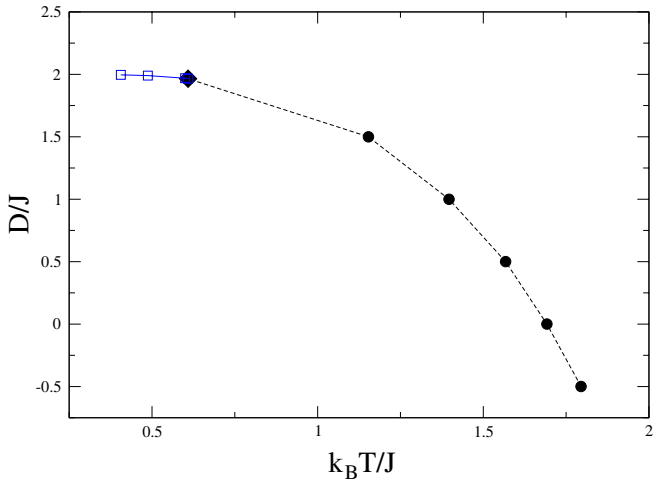

Figure 3. Phase diagram of the BC model, D/J versus kT/J. Full-circles connected by the dashed line show the second-order critical line, which meets the first-order line (open squares connected by the full line) just at the tricritical point (full diamond). For the tricritical point, one has $k_B T_t/J \simeq 0.6090$ and $D_t \simeq 1.965$. From [64].

sub-lattice is ferromagnetic, while it is antiferromagnetic for spins belonging to different sub-lattices. The Hamiltonian with an external field is

$$H = -\sum_{\langle i,j\rangle} S_{i,j}(J_1 S_{i+1,j} - J_2 S_{i,j+1} + h), \qquad (3.9)$$

where $S_{i,j} = \pm 1$ and h is the field. The phase diagram in the temperature-field plane displays a variety of critical points, depending on the ratio of coupling constants J_1/J_2. Above a critical value, the phase diagram has a tricritical point between a second-order and a first-order line [60]. Both lines indicate transitions between an ordered antiferromagnetic phase and a paramagnetic one, the OP being the staggered magnetization $M = (m_1 - m_2)/2$ (m_i is the magnetization of sub-lattice i). The second-order line and the tricritical point were studied for the case $J_1/J_2 = 1$ through STCD [66] by fixing the external field at the critical point and taking the temperature as the control parameter. The critical exponents ν and z were found to be Ising-like and almost independent of temperature and field along the second-order transition line, up to a neighbourhood of the tricritical point ($\frac{k_B T_c}{J_1} = 0.878(2)$, $\frac{h_c}{J_1} = 1.932(4)$). On the other hand, the value β was affected by the presence of the tricritical point, showing a crossover between critical Ising-like and a different universality [66].

Also studied by STCD is the double critical end-point (DCE) of the BC spin-3/2 model, where $S_i = \pm 1/2, \pm 3/2$. DCEs occur when two critical lines end simultaneously at a first-order phase boundary, and consequently two critical phases coexist (see figure 2(*b*)). For $D \neq 0$, this model presents four possible ferromagnetic ordered phases: two symmetric phases (called F_{+3} and F_{-3}) where the spins take predominantly values $S_i = \pm 3/2$ and two antisymmetric phases (F_{+1} and F_{-1}) where $S_i = \pm 1/2$. In the T–D plane, the four phases coexist along a line that extends from $T = 0$ and $D = dJ$ up to the DCE at $(\frac{k_B T_d}{J}, \frac{D}{J}) = (0.593\,74(7), 1.986\,47(5))$ [67]. Based on the calculated value of ν at the DCE, Plascak and Landau [67] concluded that this point belongs to the same universality class as the 2D Ising model. On the other hand, Grandi and Figueiredo [68] found ν and z taking the values of the 2D Ising model, but the exponent $\beta \sim 0.077$, and concluded that the DCE is not in the same universality class. The second-order transition between the ferromagnetic and paramagnetic phases was found to be Ising-like.

3.1.4. Topological effects on STCD scaling. Critical exponents depend, as is well known, on the dimension of the space in which the model is defined. Also well known is that fractals can be characterized by a dimension that is non-integer. It is thus interesting to explore the critical behaviour of systems defined on fractal substrates. Non-integer dimensions can be analysed with an RG treatment; it is found that at criticality, the exponents depend only on the dimension of the substrate *provided that translational invariance holds.* However, fractals that are built iteratively from a generating cell are not translationally invariant, and the topological details of the generating cell are present at any scale. In this case, the critical exponents depend also on the connectivity, ramification order and lacunarity of the fractal, and the behaviour is said to be 'weakly universal' [69, 70].

The critical behaviour of several models over fractal substrates with finite ramification order (i.e. where the number

Table 6. Critical parameters and critical exponents of the BC S-1 model obtained by STCD scaling, as reported in [59].

D/J	k_BT/J	β	$1/\nu$	z	θ
Critical points					
0	1.6950	0.134(2)	0.97(2)	2.106(2)	0.194(3)
−3	2.0855	0.125(2)	0.99(1)	2.128(2)	0.193(5)
−5	2.1855	0.125(4)	0.99(3)	2.139(2)	0.187(5)
Tricritical point					
1.9655	0.610	0.0453(2)	1.864(6)	2.215(2)	−0.53(2)

Table 7. Critical temperatures, critical exponents (β, γ, ν, θ, and z) and effective dimensions obtained by means of STCD scaling for the different fractal sets [17]. The Hausdorff dimensions d_H of the corresponding fractals are also indicated. More details are given in the text.

Fractal	d_H	$\frac{k_BT_c}{J}$	β	γ	ν	θ	z	d_{ef}
$SC_a(5,1)$	1.975	2.067(2)	0.122(4)	1.84(4)	1.04(3)	0.193(2)	2.30(6)	1.99(5)
$SC_a(3,1)$	1.893	1.495(5)	0.121(5)	2.22(1)	1.32(3)	0.1815(6)	2.69(6)	1.86(4)
$SC_a(4,2)$	1.792	1.10(1)	0.068(3)	3.1(2)	1.72(9)	0.181(2)	3.59(1)	1.94(7)
$SC_a(5,3)$	1.723	0.83(2)	0.016(1)	2.9(3)	1.51(7)	0.162(29)	4.97(3)	1.94(15)
$SC_a(6,4)$	1.672	0.70(5)	0.009(1)	2.9(4)	1.5(2)	0.125(5)	5.2(5)	2.0(3)
$SC_b(5,3)$	1.723	0.765(5)	0.048(1)	2.5(1)	1.45(5)	0.163(1)	3.19(7)	1.79(7)
$SC_b(7,4)$	1.797	0.94(1)	0.0657(9)	2.62(14)	1.36(4)	0.188(2)	3.16(8)	2.0(1)
$SC_b(9,5)$	1.832	1.035(2)	0.074(2)	2.18(8)	1.20(4)	0.192(1)	2.70(7)	1.94(7)
$SC_c(3,1,2)$	1.934	1.706(4)	0.111(3)	2.14(12)	1.13(5)	0.185(3)	2.4(1)	1.90(10)
$SC_c(4,2,2)$	1.861	1.451(1)	0.109(3)	2.6(1)	1.48(7)	0.181(3)	2.27(9)	1.79(15)

of links that must be cut to separate an arbitrary part of the whole fractal is finite) has been solved exactly, showing that the critical point is trivially located at zero temperature [71, 72]. Thus studies of second-order phase transitions on fractals are restricted to those with infinite ramification order, such as the Sierpinski carpet. In this case, a finite-size scaling analysis is difficult because scaling corrections are very strong and become more severe when the dimension decreases towards one and when the lacunarity increases [73, 70]. For this reason, STCD becomes an interesting alternative to investigate critical behaviour.

It is important to note that when the fractal exhibits *discrete* scale invariance (DSI), the dynamic scaling laws are different from the translational-invariant case. DSI means that the fractal is scale-invariant only between scales whose ratio is an integer power of the fundamental scaling ratio [74]. For deterministic fractals, the fundamental scaling ratio is the size of the generating cell, b. In the time domain, DSI manifests in the appearance of log-periodic oscillatory deviations from a power-law [16, 17, 75]. The scaling of the OP must thus be written as

$$M(t) = Ct^{\theta} F\left(\phi + \frac{\log t}{\log t^*}\right), \tag{3.10}$$

instead of equation (2.3), where C and ϕ are constants and $F(x)$ is a periodic function of period one, usually approximated by a truncated Fourier expansion. Similar corrections apply to the other quantities listed in table 1. Time- and space-DSI are linked by $t^* = b^z$, where t^* is the fundamental time-scaling ratio [16, 75]. Thus one can determine the dynamic exponent z from the logarithmic period ($\log t^*$) of the measured oscillation.

Table 7 summarizes the STCD results corresponding to the Ising model in various infinitely ramified fractal substrates called Sierpinski carpets SC(b, c) [17]. The SC(b, c) are constructed as follows. A square is segmented into b^2 sub-squares, and c^2 of them are removed. This segmentation process is iterated on the remaining sub-squares to, give a Hausdorff dimension $d_H = \log(b^2 - c^2)/\log(b)$. As a consequence, it is possible to vary the dimension by only changing b and c, and to obtain fractals with different lacunarities by the use of different hole distributions. In this way, in the $SC_a(b, c)$ set the c^2 sub-squares are removed from the centre of the generating cell (see figure 5(a)) and in the $SC_b(b, c)$ set they are removed in the alternate way, shown in figure 5(b). In the low lacunary set $SC_c(b, c, l)$, the generating cell is implemented as follows. A square is segmented into l^2 sub-squares, and in each sub-square one makes the same segmentation used in the $SC_a(b, c)$ (see figure 5(c)); consequently, the Hausdorff dimension is given by $d_H = \log(l(b^2-c^2))/\log(lb)$. For example, figure 4 shows the critical evolution of the magnetization, its logarithmic derivative at the critical point and the second-order Binder cumulant, after annealing the ground state, for the Sierspinki carpet $SC_a(5, 3)$ substrate (see below).

Note that the Hausdorff dimension d_H is different from the dimension obtained from the scaling laws in the STCD regime (called effective dimension d_{eff}). It is d_{eff} the dimension that verifies the hyperscaling law ($d_{eff}/z = 2\beta/\nu z + \gamma/\nu z$), at least for $d_H < 2$. Furthermore, the critical temperature obtained for the $SC_a(b, c)$ set follows a power law, with d_H suggesting $d_H = 1$ is the lower critical dimension. Finally, the observed behaviour of the dynamic exponent z implies that the slowdown of the dynamics is enhanced when the Hausdorff dimension decreases.

3.1.5. Disorder effects. The question of how *quenched disorder* (meaning that coupling constants are random variables that do not change during the system's time evolution)

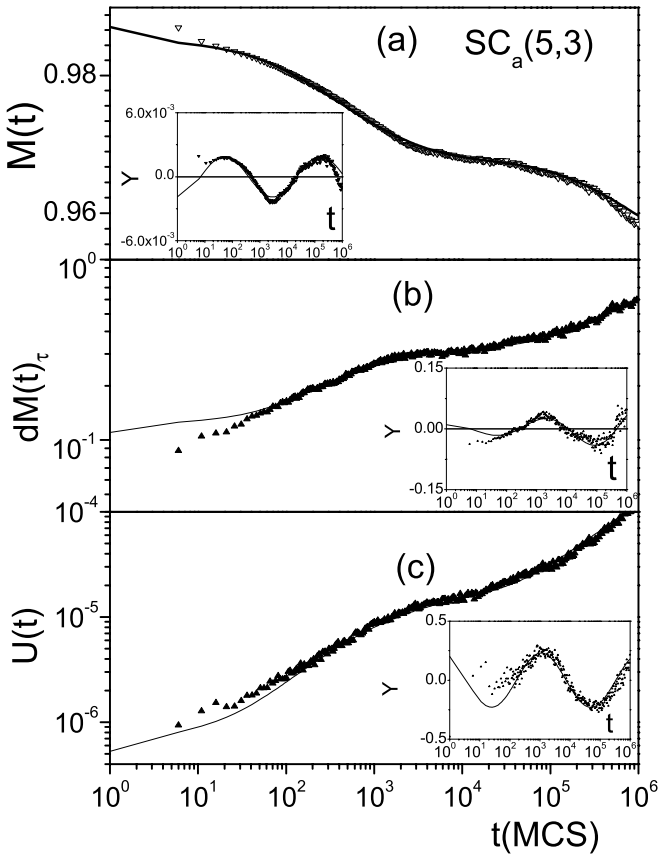

Figure 4. Time evolution of (a) magnetization, (b) logarithmic derivative of the magnetization with respect to the reduced temperature evaluated at the critical point ($dM(t)_\tau$) and (c) second-order Binder cumulant ($U(t)$) after annealing the ground state at the critical point, for the SC$_a$(5, 3). The insets show the oscillation shape obtained by subtracting and normalizing by the fitted power law.

affects the stability of long-range order is a long-standing one (see, e.g., [8, chapter 8] and references therein). An important issue is how disorder influences critical behaviour, in particular whether it changes the universality class. Strong universality means that the critical exponents are unchanged, and that disorder only introduces logarithmic corrections. The form of the scaling corrections (whether logarithmic or stronger) is of interest. In particular, STCD scaling is modified when quenched disorder is introduced.

The models we discuss here are Potts- or Ising-like, defined by

$$H = -\sum_{\langle i,j\rangle} J_{ij}\delta_{S_i S_j}, \tag{3.11}$$

with different probability distributions $P(J_{ij})$ for the couplings J_{ij}. In this section, we consider systems with non-competitive interactions (i.e. where all couplings have the same sign). Spin glasses (where frustration arises because competing ferromagnetic and antiferromagnetic interactions appear randomly) are discussed in section 3.3.

In the *site-diluted* Ising model, some sites are randomly suppressed from the Hamiltonian, corresponding to random couplings defined by

$$J_{ij} = J\epsilon_i\epsilon_j, \qquad P(\epsilon_i) = p\delta(\epsilon_i - 1) + (1-p)\delta(\epsilon_i), \tag{3.12}$$

where p thus represents the site concentration. The STCD of this model was studied by da Silva *et al* [76] on the square lattice for $0.7 < p < 1.00$. The static exponents β and ν were found to be compatible with the standard 2D Ising case, thus supporting strong universality for the statics (as also found in [77]). On the other hand, evident breakdown of universality was observed in the dynamics, with z and θ changing by a factor of two in the p range studied. The 3D case was recently studied for weak dilution ($p = 0.8$ and 0.95) [78]. The critical exponents were obtained through STCD using scaling corrections of the form $M(t) \propto t^{-\theta}(1 + bt^{\omega/z})$. The obtained exponents support the strong universality scenario.

The *random-bond* case corresponds to a bimodal distribution $P(J_{ij}) = p\delta(J_{ij} - J) + (1-p)\delta(J_{ij} - rJ)$. The 'strength of randomness' or 'disorder amplitude' $0 \leqslant r < 1$ is a fixed parameter and here p is the relative concentration of bond types. The 2D random-bond Ising model was studied in [79] for $p = 1/2$. This model has weak universality [79]: exponents ν and γ depend on the strength of randomness. To obtain the non-equilibrium critical exponents of the autocorrelation function and the second moment of the magnetization when the system is quenched from the disordered state, the following corrections to STCD scaling were proposed [79],

$$O(t) \propto t^{-\alpha}(1 - bt^{-c}), \tag{3.13}$$

where $O(t)$ is the relevant observable (say one of those listed in table 1), α is the corresponding STCD exponent, and c and b are constants. These corrections allow us to obtain the dynamic exponent z in good agreement with that estimated by measuring the relaxation from the ordered state.

Yin *et al* [80] studied the 2D random-bond $q = 8$ Potts model for $p = 1/2$ and $r = 3$, 4 and 10 (for these values of r the transition is second order, while for $r < r_c = 1.3$ there is evidence of a first-order transition [80]. For this value of p, the critical point can be computed exactly [80]. The results for β/ν show little dependence on the disorder amplitude. In contrast, $1/\nu$ depends on r, as has also been found for the 3-state Potts [81]. The dynamic exponent z is also r-dependent, and much larger than in the 2D Ising model. For θ Yin *et al*, find $\theta = 0.061(4)$ for $r = 10$, a value much smaller than $\theta = 0.203(3)$ reported previously [82], apparently indicating corrections to scaling induced by the disorder.

The STCD of the 3D $q = 3$ Potts model was studied in [83]. In this work, the authors determined the critical value of r, $r_c = 2.3(1)$ above which the second-order transition becomes weak first order. For strong disorder ($r = 10$), the scaling corrections (3.13) were applied to the Binder cumulant and its logarithmic derivative in order to obtain the critical exponents. The results support the universality of the phase transition with respect to the disorder [83].

When the disorder amplitude is taken as $r = 0$ (i.e. some interactions are randomly removed), the models are called *bond-diluted.* The parameter p then represents the bond

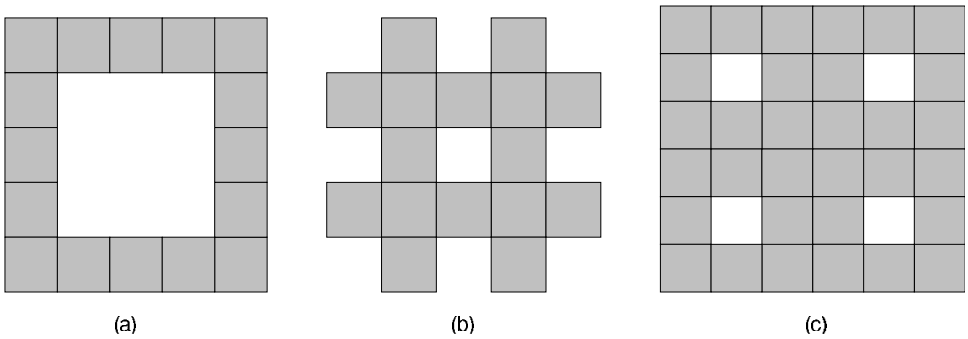

Figure 5. Some examples of the generating cells of the Sierpinski carpet sets used in [17]: (*a*) $SC_a(5, 3)$, (*b*) $SC_b(5, 3)$ and (*c*) $SC_c(3, 1, 2)$.

concentration. The STCD of the 3D bond-diluted $q = 4$ Potts model was studied by Yin *et al* [84] using a non-equilibrium reweighting [85]. They studied in particular the tricritical region, found for $p = 0.74$ (for higher p the transition is first order, and second order for lower p). They computed the critical exponents for the continuous transition (at $p = 0.44$, 0.56 and 0.68), finding values in agreement with [86, 87]. The exponents z, λ and β/ν are concentration-dependent, the latter non-monotonically. For $1/\nu$, only a weak dependence was detected.

Finally, Zheng *et al* [88] have studied an anisotropic bond-diluted Ising defined by

$$H = -J_0 \sum_{i,j} S_{i,j} S_{i,j+1} - \sum_{i,j} J_j S_{i,j} S_{i+1,j}, \tag{3.14}$$

where the coupling among columns J_j is random with probability $P(J_j) = (1 - p)\delta(J_j) + p\delta(J_j - J_0)$. For bond concentration $0 < p \leqslant 1$, long-range order exists at a non-trivial T_c. For strong dilution ($p \ll 1$), the scaling relations corresponding to relaxation from the ordered state must be corrected in order to obtain critical exponents independent of disorder and initial state, and comparable to those of the 2D Ising model [88]. The corrections are based on the critical behaviour of the correlation length [89],

$$\xi(t) \propto \frac{t^{1/z}}{[1 + C_0 \ln(t)]^{1/z'(p)}}, \tag{3.15}$$

where for $p = 1$, $1/z'(p) = 0$. In this way, the magnetization scaling can be written [79]

$$M(t) \propto \frac{t^{1/z}}{[1 + A(p) \ln(t)]^{B(p)}}, \tag{3.16}$$

where $A(p)$ and $B(p)$ are functions that depend only on the bond concentration. The 3D case was studied by Parisi *et al* [90]. In order to obtain the dynamic exponent z independently of the disorder, the authors proposed the following correction to the susceptibility at the critical point,

$$\chi(t) = A(p)t^{1/\nu z} + B(p)t^{1/\nu z - w/z}, \tag{3.17}$$

where w is the correction scaling exponent that corresponds to the largest irrelevant eigenvalue of the dynamic renormalization group [90, 91].

3.1.6. Surface effects. Real systems are always bounded by surfaces or interfaces between different phases. These break translational invariance and affect the nearby coupling constants, and are thus expected to influence the physical properties of the system, including the universal features. The resulting critical behaviour depends only on general properties of the surface and in turn can be classified in different *surface* universality classes, stemming from the same bulk universality class. They are in general characterized by surface critical exponents, different from the corresponding bulk ones (see, for example, the reviews [92–94]). Space and time correlation functions involve new exponents β_1/ν and λ_1, respectively [95]. On the other hand, there are no independent dynamic critical surface exponents [95–98] (the exponents z and x_0 remaining unchanged). In this context, several studies of the STCD of surfaces [99–106] and thin films [107, 108] have been performed.

Ritschel and Czerner [99] generalized the STCD treatment to a magnetic system with a free surface, and derived the dynamic scaling form for the dynamic relaxation. The presence of a surface influences the dynamics of a particle when the non-equilibrium (growing) correlation length ξ becomes of the order or larger than the distance from the particle to the surface, y [99]. As a result, the magnetization close to the surface ($y \ll \xi(t)$) scales as

$$M(y, t, m_0) \sim y^{(\beta_1 - \beta)/\nu} t^{\theta_1}, \tag{3.18}$$

with $\theta_1 = (x_0 - \beta_1/\nu)/z$. The exponent β_1 is the static exponent of the surface magnetization [93]. Similarly, the autocorrelation function $A(t)$ (equation (2.8)) decays with time as

$$A(t) \sim y^{2(\beta_1 - \beta)/\nu} t^{-\lambda_1}, \tag{3.19}$$

where $\lambda_1 = d/z - \theta_1$ [99].

A simple model used to study surface dynamics is the semi-infinite Ising model,

$$H = -J_s \sum_{i,j \in \text{surface}} S_i S_j - J_b \sum_{i,j \in \text{bulk}} S_i S_j, \tag{3.20}$$

where J_s and J_b are the surface and bulk coupling constants. The first sum runs over pairs of nearest-neighbour surface spins, whereas the second sum includes pairs with at least one spin belonging to the bulk. In two dimensions, surface and bulk order at the bulk critical temperature T_c independently

Table 8. Critical exponents θ_1 and $\lambda_1 = d/z - \theta_1$ of the semi-infinite Ising model corresponding OT and ST, as obtained by STCD scaling [99, 102, 106]. Theoretical predictions (T) are also reported [102, 106].

	β_1/ν (T)	θ_1	$\theta_1(T)$	λ_1	λ_1 (T)
2D OT	0.5	0.015(3)	0.014		
3D OT	1.26	−0.255(4)	−0.255	2.10(1)	2.10
3D ST	0.376	0.179(4)	0.178	1.16(2)	1.22

of the surface coupling. In three dimensions, however, the surface behaviour depends on the ratio J_s/J_b [109]. There are three cases: (i) extraordinary transition (ET), where the surface orders at a temperature higher than T_c, when $J_s/J_b > r_{sp}$, with $r_{sp} = 1.5$ for a cubic lattice; (ii) ordinary transition (OT), where bulk and surface order at T_c, for $J_s/J_b < r_{sp}$; and (iii) when $J_s/J_b = r_{sp}$ the two critical lines meet at a multicritical special transition (ST). The values of the exponents obtained from STCD scaling corresponding to OT and ST are quoted in table 8 and compared with the expected theoretical values.

Another (2D) semi-infinite Ising model is the Hilhorst–van Leeuwen model, which has an extended surface defect where the coupling constants have a constant value (J_1) in the direction parallel to the surface but in the perpendicular direction depend on the distance y to the surface as $J_2(y) = \Lambda y^{-\omega} + J_2(\infty)$. Depending on the interaction parameters, different behaviour results: (i) when $\omega > 1$ the model behaves as the semi-infinite Ising model described above; (ii) $\omega < 1$ and $\Lambda > 0$ result in OT; (iii) when $\omega = 1$ and $\Lambda < 1$ non-universal behaviour is obtained where the scaling exponent of the space correlations is $\beta_1/\nu = \frac{1}{2}(1-\Lambda)$. The last regime was studied by means of STCD; the exponents θ_1 and λ_1 obtained are given in table 9 together with the corresponding theoretical predictions [102, 106].

In summary, in a spatially inhomogeneous system, such as at a free surface, the local critical behaviour is generally different from that in the bulk and one must introduce local critical exponents. The exponents that govern the short-time dynamics can be expressed in terms of scaling relations between other known critical exponents. A similar situation arises when inhomogeneities are caused by defects (see section 3.1.7).

3.1.7. Non-universal critical behaviour. We conclude section 3.1 considering other cases with non-universal criticality studied through STCD.

The 2D Ising model with a defect line displays non-universal critical behaviour due to inhomogeneity, and its STCD has been studied in [102, 110]. Two types of defect lines were considered: a chain defect where the spins along the line have different coupling constants, and a ladder defect where different coupling constants connect spins belonging to neighbouring columns. In both cases, analytic expressions for the exponent β_1/ν as a function of the ratio of coupling constants are reported in the literature [102, 110]. For the first case, Simões *et al* [110] have verified by means of STCD that β_1/ν along the defect line depend on the ratio of the couplings, while x_0 and z remain unaltered. Similar results were reported by Pleimling and Tglói [102] (see table 10).

Table 9. The Hilhorst–van Leeuwen critical exponents obtained through STCD as a function of the parameter Λ for $\omega = 1$ (see text). Theoretical predictions (T) are also included [102, 106].

Λ	β_1/ν (T)	θ_1	$\theta_1(T)$	$d/z - \theta_1$	$d/z - \theta_1$ (T)
0.75	0.125	0.188(3)	0.187		
0.50	0.250	0.131(3)	0.130	0.84(1)	0.85
0.25	0.375	0.076(4)	0.072	0.96(1)	0.96
−0.25	0.625	−0.045(2)	−0.044	1.22(2)	1.19
−0.50	0.750	−0.107(4)	−0.101	1.30(2)	1.31
−0.75	0.875	−0.157(3)	−0.159		
−1	1.000	−0.214(5)	−0.217		
−1.25	1.125	−0.29(1)	−0.274		
−1.50	1.250	−0.37(3)	−0.332		

Table 10. Critical exponent θ_1 obtained from STCD for the 2D Ising model with a ladder defect line as a function of the coupling constant along the line (J_l). The theoretical predictions (T) of β_l/ν and θ_l are also included [102].

J_1	β_1/nu (T)	θ_1	$\theta_1(T)$
0.2	0.376	0.072(1)	0.071
0.4	0.278	0.118(1)	0.116
0.6	0.208	0.148(1)	0.148
0.8	0.159	0.171(1)	0.171
1.0	0.125	0.188(1)	0.187
1.2	0.101	0.199(1)	0.198
1.4	0.085	0.208(2)	0.206

Non-universality was also observed in the Ising model with competing first- and second- neighbour interactions [111–113]. The Hamiltonian is

$$H = -J_1 \sum_{\langle i,j \rangle} S_i S_j - J_2 \sum_{\langle\langle i,j \rangle\rangle} S_i S_j, \qquad (3.21)$$

where $\langle i, j \rangle$ and $\langle\langle i, j \rangle\rangle$ denote sums over first- and second-neighbours. At $T = 0$, the system is ferromagnetic for $-J_2/J_1 < 1/2$ and antiferromagnetic for $-J_2/J_1 > 1/2$ [111]. In the plane of reduced temperature kT/J_1 versus coupling constant ratio $-J_2/J_1$, the phase diagram has two critical lines separating the ferromagnetic and antiferromagetic phases from the paramagnetic phase. The exponents along the ferromagnetic–paramagnetic line belong to the 2D Ising universality class, whereas along the antiferromagnetic–paramagnetic line they are non-universal, and they depend on the coupling constant ratio [111, 112]. Alves and Drugowich de Felicio [113] used STCD to show that θ, β and ν increase with $-J_2/J_1$, eventually reaching their known Ising values. However, the dynamic exponent z did not show a clear dependence, which prevented conjecture about its universality.

Another case with non-universal critical behaviour studied with STCD is the stacked-triangular XY antiferromagnet (XY STA), which is the simplest model with frustration induced by geometry. Perturbative RG calculations predict a second-order transition [114, 115], but non-perturbative RG methods point to a weak first-order one [116, 117]. MC simulations indicate a second-order phase transition with a set of critical exponents associated with a new universality

class [118]. On the other hand, the XY STA model with rigid constraint (STAR), where the structure of the ground state is locally imposed at all temperatures, exhibits a first-order phase transition despite it belonging to the universality class of the STA XY [119]. In order to study the effect of the rigidity, Bekhechi *et al* [120] have proposed a modified version of XY STA model defined by

$$H(r) = -\sum_{\langle i,j\rangle} J_{ij} S_i S_j + r \sum_{\text{plaquettes}} (S_A S_B S_C)^2, \qquad (3.22)$$

where the J_{ij} are antiferromagnetic, the subscripts A, B, C label the three sub-lattices on the corners of each elementary triangle, and 'plaquettes' refers to the disconnected triangles. The parameter r imposes the constraint to the short wavelength fluctuations of the order parameter and allows a continuous change from STA to STAR when varying from 0 to ∞. For $r > 1$, there is a first-order transition, but for $r < 1$, critical behaviour with r-dependent exponents is observed. STCD scaling results [120] indicate that the phase transition is accompanied by hysteresis for several values of r, which suggests that the transition of STA XY is weakly first order in agreement with the non-perturbative RG arguments.

3.2. Kosterlitz–Thouless transitions

Kosterlitz–Thouless (KT) transitions [121] are continuous phase transitions in which the correlation length diverges exponentially when the transition temperature T_{KT} is approached from above ($\xi \sim e^{b/\epsilon^{\nu}}$ when $T \to T_{KT}^{+}$, with $\epsilon = T - T_{KT}/T_{KT}$). The susceptibility diverges as $\chi \sim \epsilon^{2-\eta}$ with $\eta = 0.25$ [122]. Below T_{KT}, ξ and χ are always infinite; in this sense it is said that the system is 'always critical'. Another remarkable aspect is that there is no symmetry breaking at $T < T_{KT}$, with quasi-long-range ordering present in the system.

KT transitions occur in several widely studied 2D models with short-range interactions: the XY model, its fully frustrated version (FFXY), and the 6-state clock model. The Hamiltonian of these models is given by

$$H = -J \sum_{\langle ij\rangle} f_{ij} S_i S_j = -J \sum_{\langle ij\rangle} f_{ij} \cos(\vartheta_i - \vartheta_j), \qquad (3.23)$$

where a spin is represented by a 2D vector S_i with unitary modulus or by its angle ϑ_i. In XY or FFXY, ϑ spans the interval $0 \leqslant \vartheta_i < 2\pi$, while in the 6-state clock it takes the discrete values $\vartheta_i = 2\pi/6n_i, n_i = 0, \ldots, 5$. J is the coupling constant. In the clock and XY models, $f_{ij} = 1$, while for the FFXY it depends on the particular version of the model. A simple realization for f_{ij} is given in [123], which defines a sub-lattice structure.

The KT transition for the XY was found numerically to be at $T_{KT}^{XY} = \frac{J}{k_B}0.894(5)$ [124]. The FFXY model has a KT phase transition located at $T_{KT}^{FFXY} = \frac{J}{k_B}0.4460(1)$ or $T_{KT}^{FFXY} = \frac{J}{k_B}0.440(2)$, and an Ising-like phase transition at $T_c^{FFXY} = \frac{J}{k_B}0.452(1)$ or $T_c^{FFXY} = \frac{J}{k_B}0.454(2)$ according to [125] or [126], respectively. Approximate analytic and numeric results have shown that the 6-state clock model has two KT transitions, at $T_{KT}^{1} = \frac{J}{k_B}0.645$ [127] and $T_{KT}^{2} = \frac{J}{k_B}0.92(1)$ [128].

The transition has also been studied by observing its STCD behaviour near the Kosterlitz–Thouless temperature. It has been found that if the XY, the FFXY and the 6-state clock models are started from disordered configurations with a small magnetization m_0 along the x-axis and are quenched near $T \simeq T_{KT}$, the dynamic evolution of the magnetization along the x-axis $M_x(t)$ (the y-component is zero all along the evolution) increases as a power law after the microscopic time regime [129, 130], and it is independent of both the m_0 (the magnetization $M(t) = (M_x(t), M_y(t))$ is the OP) and the dynamics employed [129]. The same happens if one considers a different sub-lattice magnetization for the FFXY model. In consequence, the dynamic behaviour of the model is universal for $M_x(t)$, although this observable is not the OP of the system because it breaks the $O(2)$ symmetry below T_{KT}. So, the exponent θ can be defined. In the $T < T_{KT}$ regime, θ increases as T decreases for the XY, FFXY and the 6-state clock models [129–131]. Also, Czerner *et al* estimated the exponents η and z in the 6-state clock model by measuring the second moment of the magnetization and the autocorrelation function, also for temperatures $T < T_{KT}$. They found that z is almost constant within error bars, while η decreases when T goes to zero [130].

If the system is started from an ordered configuration with $m_0 = 1$, the results in the XY and FFXY suggest that there is a universal power-law behaviour in the short-time regime. The initial condition is obtained by imposing an initial magnetization directed along the x-axis and equal to 1, so $M_x(t = 0) = 1$ for the XY model, while for the FFXY model $M_x(t = 0) \leqslant 1$ because of the frustrated ground state [2]. By measuring $M_x(t)$ [124] and the Binder cumulant $U(t)$ [132], the exponents η and z could be estimated for both the XY and FFXY models [124, 133]. For the XY, the calculated values of η are in accordance with those estimated theoretically at $T = T_{KT}$ [122] and numerically measured in equilibrium states for $T \leqslant T_{KT}$ [124, 133]. The same happens for the FFXY model at $T = T_{KT}$, but at $T \leqslant T_{KT}$ the values are larger than those numerically calculated in equilibrium measurements [133], due to strong finite-size effects. Furthermore, for both models, the calculated values of z remain almost constant around $z \simeq 2$ for all investigated temperatures $T \leqslant T_{KT}$ [132], and are in good agreement with the value predicted theoretically [134]. Also, the calculated values of η and z for the FFXY model suggest that the transition temperature is near $T = \frac{J}{k_B}0.440$ rather than $T = \frac{J}{k_B}0.446$, as estimated in [125].

3.3. Spin glasses

Spin glasses are systems with quenched random interactions leading to frustration and very slow approach to equilibrium at low temperatures. The early evolution of these systems has also been studied. These models exhibit a phase transition between a paramagnetic (PM) and a spin-glass (SG) phase where the spins freeze in random directions. The short-time studies of these kinds of systems are relevant because these models are generally affected by ageing phenomena, i.e. quantities will depend on the *waiting time*, that is the time

elapsed between the establishment of the initial condition and the start of measurements. This is also an issue in experimental studies.

One of the most studied SG models is the 3D $\pm J$ Ising spin glass, defined by the Hamiltonian equation (3.11) where the J_{ij} are taken equal to $\pm J$ with equal probability. Luo *et al* investigated the critical behaviour of this model in a cubic lattice, and measured the increase and dynamic exponents, θ and z [131].

The OP of the spin-glass transition is not the magnetization but the Edwards–Anderson parameter $q_{\rm EA}$, or the overlap distribution [135]. However, $q_{\rm EA}$ cannot be computed on a single configuration. Accordingly, Luo *et al* set up two replicas as follows. For a given realization of the disorder, they started from a random configuration and evolved it to generate a low energy configuration S_i^0. Then two independent replicas with small magnetization m_0 were generated by randomly setting each spin site with $S_i^0 = 1$ or -1 with probability $(1+m_0)/2$ or $(1-m_0)/2$, respectively. They then followed the evolution of the overlap

$$Q(t) = \frac{1}{L^d}\sum_i S_i^1(t)S_i^2(t), \tag{3.24}$$

where $S_i^1(t)$ and $S_i^2(t)$ represent the (independent) evolution spin i in each replica. It is expected that $Q(t)$ will increase as a power law,

$$Q(t) \propto m_0 t^{2\theta}. \tag{3.25}$$

For the Ising model, Q should behave as the second moment of the magnetization.

The evolution of $Q(t)$ was followed above, below and at the critical temperature, quoted as $T_{\rm c} = 1.175(25)\ J/k_{\rm B}$ ($k_{\rm B}$ is Boltzmann's constant) [136]. A double average is performed: over the thermal history and over disorder. It was found [131] that at $T_{\rm c}$, $Q(t)$ is a power law after a short microscopic time, and the exponent θ was estimated as $\theta = 0.085(5)$. At temperatures larger than $T_{\rm c}$, $Q(t)$ bends downwards. However, at temperatures slightly below $T_{\rm c}$, $Q(t)$ is still a power law, with a similar exponent $\theta = 0.09$, suggesting that $T_{\rm c}$ is even below that reported in [136].

The scaling relation $\lambda = d/z - \theta$ obtained for the autocorrelation function in the Ising model (see table 1) was tested. Taking $\lambda = 3.9$ [137] and θ as inputs, the dynamic exponent was obtained as $z = 6.3$, which is in good agreement with the values reported in [138–140].

A more extensive and thorough study of the same model was performed by Ozeki *et al* [141]. These authors consider ageing effects by taking into account the waiting time $t_{\rm w}$. The initial configuration was obtained starting from a state with all spins up and letting it evolve for a time interval $t_{\rm w}$ at a temperature T. Then, two identical replicas $S^1(0)$ and $S^2(0)$ are generated from it, and evolved with different realizations of the thermal bath. The order parameter is again the overlap but the $t_{\rm w}$ dependence is explicitly considered,

$$Q(t, t_{\rm w}) = \langle\langle S_i^1(t+t_{\rm w})S_i^2(t+t_{\rm w})\rangle^F\rangle^J, \tag{3.26}$$

where $\langle\ldots\rangle^F$ and $\langle\ldots\rangle^J$ mean average over thermal history and disorder, respectively. If $t_{\rm w}$ is small, the initial system will be far from equilibrium, but in the limit $t_{\rm w} \to \infty$, the system approaches equilibrium. So the short-time evolution of $Q(t, t_{\rm w})$ will depend on $t_{\rm w}$. In this way, the ansatz for the dynamical critical evolution of $Q(t, t_{\rm w})$ is

$$Q(t, t_{\rm w}) = F(t_{\rm w})t^{-\lambda}, \tag{3.27}$$

where F is an unknown function of $t_{\rm w}$. In the Ising model, λ is equal to $\beta/z\nu$ (table 1).

Ozeki *et al* investigated the critical evolution of Q in the SG and PM phases, for several $t_{\rm w}$s in the range $1 \leqslant t_{\rm w} \leqslant 10^8$. In the PM phase, $Q(t, t_{\rm w})$ decays exponentially with a characteristic thermalization time τ that depends only on T. If $t_{\rm w} < \tau$, the decay depends on $t_{\rm w}$ because the state at $t = t_{\rm w}$ is not in equilibrium. If $t_{\rm w} > \tau$, the initial state is an equilibrium state, so $Q(t, t_{\rm w})$ is independent of $t_{\rm w}$. The amplitude $F(t_{\rm w})$ (equation (3.27)) does not depend on $t_{\rm w}$ if $t_{\rm w} > 10^2$.

The local slope $\lambda(t, t_{\rm w}) = -{\rm d}\log Q(t, t_{\rm w})/{\rm d}t$ increases with $t_{\rm w}$ and diverges in the $t \gg t_{\rm w}$ regime, a consequence of the exponential decay. For $t \sim t_{\rm w}$, $\lambda(t, t_{\rm w})$ still increases with all $t_{\rm w}$s considered, and reaches a constant value independent of $t_{\rm w}$ if $t \ll t_{\rm w}$ because $Q(t, t_{\rm w})$ is in equilibrium. It is expected that $\lambda(t, t_{\rm w}) \to 0$ in the $t_{\rm w} \to \infty$ limit.

At $T = T_{\rm c}$, $Q(t, t_{\rm w})$ shows two power-law regimes, with a crossover that occurs at $t \sim t_{\rm w}$. In the first power law at $t \ll t_{\rm w}$, the amplitudes $F(t_{\rm w})$ do not depend on $t_{\rm w}$, while they do in the second ($t \gg t_{\rm w}$) regime. The local exponent does not depend on $t_{\rm w}$ in either regime.

For $T < T_{\rm c}$, $Q(t, t_{\rm w})$ reaches a finite value with some SG ordering in the $t \ll t_{\rm w}$ regime, and $\lambda(t, t_{\rm w})$ decreases with $t_{\rm w}$. Finally, if $t \gg t_{\rm w}$ $Q(t, t_{\rm w})$ shows a power-law behaviour with $\lambda(t, t_{\rm w})$ independent of $t_{\rm w}$. The increase (decrease) in λ at $T > T_{\rm c}$ ($T < T_{\rm c}$) helped us to find upper and lower bounds for $T_{\rm c}$, namely $1.0 \leqslant T_{\rm c} \leqslant 1.25$, in agreement with previous measurements in smaller lattices. Furthermore, by performing a dynamic scaling [141], the exponent of both power laws at $T = T_{\rm c}$ was estimated as $\lambda(t < t_{\rm w}) = 0.06(2)$, consistent with equilibrium measurements [137–139], and $\lambda(t > t_{\rm w}) = 0.16(2)$.

3.4. Helix–coil transition in polypeptides

The folding of proteins involves transitions between different thermodynamics states, and its mechanism is a long-standing problem in protein science. One of the most studied folding transitions is the helix–coil transition, which has been approached with several methods, including RG techniques and, recently, STCD. At high temperatures, the prevailing structure is a disordered coil, while for low temperatures one finds mostly helical structures. In the case of polyalanine, for which the infinite size limit can be defined, some evidence has been reported that it can be considered a true thermodynamic phase transition [142, 143].

The STCD of the helix–coil transition was recently studied in a MC simulation of an all-atom representation model of polyalanine chains of N residues, $({\rm Ala})_N$ [144, 145]. The order parameter of the transition is

$$q_{\rm H} = 2\langle n_{\rm H}(T)\rangle/(N-2) - 1, \tag{3.28}$$

where $\langle n_H \rangle$ is the average number of helical residues. A residue is defined helical if its backbone dihedral angles (ϕ, ψ) take values in the range $(-70^\circ \pm 30^\circ, -37^\circ \pm 30^\circ)$, and the residue is hydrogen bonded. The dynamics were studied starting from the completely ordered phase ($q_H = 1$). At the critical temperature, the time evolution of q_H is expected to be described by equation (2.9). The different exponents were determined with the aid of the relations for the relaxation of the second cumulant and logarithmic derivative of M for the ordered case (table 2).

For $(Ala)_N$, the STCD-determined critical temperature is N-dependent. The estimated values are lower than the estimates from the peak in the specific heat, the discrepancy due to the finite size of the system (the values of N were 10, 20, 30 and 40). For all N, however, the exponents are the same, namely $\beta/\nu z = 0.30$, $1/\nu z = 0.77$ and $d/z = 1.10$ [145]. These values rule out a first-order transition.

The study has also been extended to a model of peptide fragment PTH(1–34), corresponding to residues 1–34 of the human parathyroid hormone. Unlike homopolymers, this protein has a unique sequence, so that critical exponents cannot be determined by other techniques because it is not possible to define the infinite chain length limit. In this case, the nature of the transition had not been established. The results show a power-law behaviour with the same exponents as in the previous case. Since in PTH(1-34) the side chains differ for each residue, this result suggests that the order of the transition does not depend on the side chains. It is also independent of the number of residues. In summary, it seems that the helix–coil transition in protein-like polymers is universal.

These results show that STCD opens a new way to characterize the helix–coil transition, and in particular that it is a very useful tool to apply to proteins where the infinite chain length limit is not meaningful.

3.5. Dynamics of damage spreading in confined geometries

Damage spreading is a method for studying the propagation of perturbations in lattice systems, and it has been applied to the Ising magnet, spin glasses, Potts model, cellular automata and biological models (see the recent review [146]). It consists in simulating the system by starting with two initial configurations $S^A(T)$ and $S^B(T)$ differing from each other only in a small number of sites. Then both configurations are allowed to evolve under the same realization of the thermal noise (in Monte Carlo terms, one uses the same sequence of pseudo-random numbers for both configurations). Thus, at time t the difference between S^A and S^B will be due only to the small initial perturbation, or *damage*, introduced at $t = 0$. The Hamming distance is used as a measure of the damage $D(t)$ [147],

$$D(t) = \frac{1}{2N} \sum_{l}^{N} |S_l^A(t, T) - S_l^B(t, T)|. \tag{3.29}$$

The sum runs over the whole lattice, and l labels the sites. $S^A(t, T)$ is taken as an equilibrium configuration at temperature T, while $S^B(t, T)$ is the damaged configuration [147, 148]. If the perturbation introduced in S^B is small ($D(t = 0) \sim O(1/N)$, N being the number of sites), there are two possible scenarios: (i) the perturbation disappears after some time and $D(t \to \infty) \to 0$ in the thermodynamic limit or (ii) $D(t \to \infty)$ is finite, and the perturbation is relevant. Thus there is a transition between a state where damage heals and a state where the perturbation propagates throughout the system. This is a continuous and irreversible critical transition [146], known as the *damage spreading* (DS) transition. Precisely at the transition temperature, the damage heals, but (analogous to the OP in second-order transitions) at short times the damage increases as a power law,

$$D(t) \sim t^{\theta_D}. \tag{3.30}$$

Two quantities are of interest in describing the damage dynamics. One is the damage survival probability $P(t)$, defined as the probability of finding non-zero damage at time t. It is expected that at the critical point $P(t)$ should decay as a power law [149],

$$P(t) \propto t^{-\delta}. \tag{3.31}$$

The second quantity describes the spreading of damage in space when starting with an initially localized perturbation. Then we can define

$$R^2(t) = \left\langle \sum_{l}^{N} |S_l^A(t, T) - S_l^B(t, T)| r_n^2 \right\rangle_B \propto t^{z^*}, \tag{3.32}$$

where r_n^2 is the squared distance from n to the site of the original (local) perturbation, z^* is a critical exponent and $\langle \ldots \rangle_B$ means an average over different realizations of the thermal bath.

The DS transition temperature T_D depends on the dynamics, and need not coincide with the critical temperature(s) of thermodynamic transition(s) that the model might exhibit. For instance, in the 2D Ising model with Glauber dynamics, $T_D = 0.992(2)T_c$ [150] (T_c is the Onsager critical temperature). The universality class of the DS transition is still an open question. Grassberger [151] conjectures that it belongs to the directed percolation (DP) universality class [152–154] if T_D does not coincide with a thermodynamic critical transition. The conjecture seems to hold for the Domany–Kinzel cellular automata [151], the 2D Ising model with Swendsen–Wang dynamics [155] as well as the deterministic cellular automata with small noise [156]. However, a different behaviour has been observed in the Kauffman model [157, 158] and the Ziff–Gulari–Barshad (ZGB) model in 2D [159] (see also [146]).

STCD has been applied to DS in the Ising model at the Onsager temperature with heat-bath dynamics in $d = 2$ and 3 by Grassberger [160]. The exponent θ_D (3.30) was found to be $\theta_D = 0.191(3)$ ($d = 2$) and $\theta_D = 0.104(3)$ ($d = 3$). The damage survival probability exponent (3.31) was found to be $\delta \approx 0.9$ ($d = 2$) and $\delta \approx 1.1$ ($d = 3$). For random independent initial configurations (i.e. half of the spins damaged on average), a decrease in damage is observed and a power law with an exponent $\theta'_D = 0.43(2)$ ($d = 3$).

A more recent study [161] applied the STCD technique to study DS in the 2D Ising model with Metropolis dynamics. In this work, the starting configurations S^A were chosen with

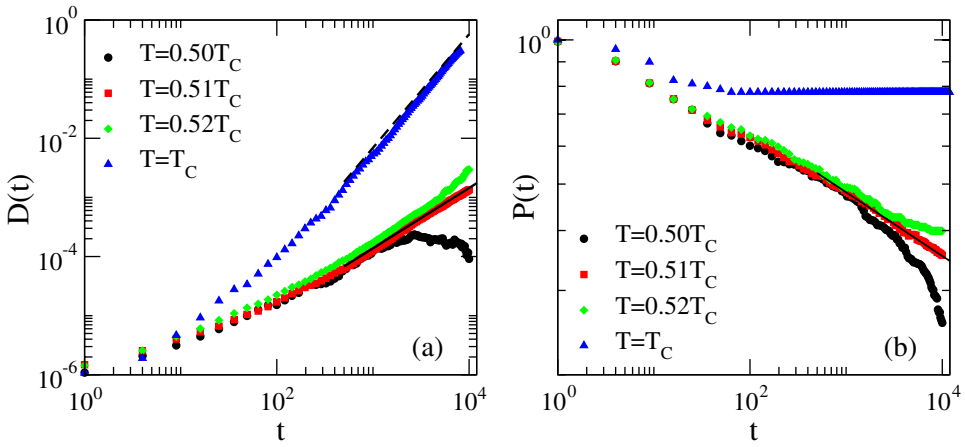

Figure 6. Plots obtained for a lattice of side $L = 2048$ and different temperatures T as indicated in the figure. (a) Damage ($D(t)$) versus t. The dashed line (corresponding to $T = T_c$) has slope $\theta_D(L = 2048) = 1.91$ and the full line ($T = T_D \approx 0.51T_c$) has slope $\theta_D = 1.026(3)$. (b) Survival probability of damage ($P(t)$) versus t. As can be observed, at $T = T_c$, $P(t)$ reaches a stationary value corresponding to $\delta = 0$. The full line ($T = T_D \approx 0.51T_c$) has slope $\delta = 0.133(1)$. (Color online.)

initial magnetization strictly equal to zero (corresponding to $T = \infty$). Suddenly, the system is quenched at a certain temperature T, and the damage is applied to the replica configuration S_B by flipping N_0 spins. In this way, the initial damage $D_0 = 1/N_0$ is strictly equal to the initial magnetization m_0.

It was found that the value of the exponent θ_D at the Onsager temperature depends on the initial magnetization m_0. To establish the value of θ_D in the $m_0 \to 0$ and $L \to \infty$ limits, an epidemic study was carried out, damaging by flipping a single spin, so $m_0 = 1/L^2$ (triangles in figure 6(a)). After appropriate finite-size scaling, the result is $\theta_D(L \to \infty, m_0 \to 0) = 1.915(3)$. This exponent is much larger than the exponent for the initial increase for the magnetization $\theta = 0.197$ [2]. The same study considered the damage survival probability, and found that at $T = T_c$, $P(t)$ reaches a stationary value, corresponding to $\delta = 0$ (triangles in figure 6(b)). This result is in agreement with that reported by Montani and Albano [162] in the 2D Ising Model with Glauber dynamics.

Furthermore, there is another (lower) temperature where both $D(t)$ and $P(t)$ behave as power laws. This happens at $T_D = 0.51(1)T_c$, and the corresponding exponents were calculated to be $\theta_D = 1.026(3)$ and $\delta = 0.133(1)$ (see figure 6). Also, $z^* = 1.74(3)$ was found at T_D.

The values of these exponents differ from those reported by Grassberger for the Ising model with heat-bath dynamics at T_c [160]; however, it is worth mentioning that both systems are quite different. In fact, here the damage is introduced in a completely uncorrelated configuration that is suddenly quenched at a temperature T, and subsequently the damage starts to evolve with standard Metropolis dynamics. Therefore, a completely different scenario is expected. Furthermore, the critical behaviour is not observed at T_c—or close to it, as usual—but at a lower temperature $T \approx 0.51T_c$.

3.6. First-order transitions

If the first derivatives of the free energy are discontinuous at the transition point, the transition is called first order. In this case, when the free energy curves of the high- and low-temperature phases intersect (i.e. at the transition), they have different slopes, so that both stable and metastable states exist in some interval around the transition. If the transition temperature is T_c, then when T is varied smoothly from $T > T_c$ to $T < T_c$, the system remains in the phase corresponding to thermodynamic equilibrium at $T > T_c$. When the phase survives despite being carried out beyond its thermodynamic 'homeland', it is called *metastable*. The metastable phase has a finite (though possibly very long) lifetime, but it is no longer observed if $T < T_{sp}$. The temperature T_{sp} is called the *spinodal temperature.*

In far-from-equilibrium situations, first-order *irreversible* transitions are also characterized by a discontinuity in the relevant observables when the system passes from one phase to the other. These transitions display the same characteristics as their equilibrium counterpart, namely metastability, hysteresis and spinodals [163, 164]. Due to these effects, the determination of the transition point becomes very difficult. The STCD technique can avoid the influence of the metastable states and hysteresis, e.g. using a mixed-phase initialization, which is a configuration consisting of both the ordered and disordered states separated by a flat interface. The dynamic evolution of the OP is recorded, and a local exponent is evaluated. The critical temperature is then identified as that where a decreasing trend of the OP in the $t \to \infty$ limit (for the disordered phase, $T > T_c$) changes into an increasing trend (for the ordered phase, $T < T_c$). This method has been successfully tested for the Potts model with $q = 20$ and $q = 5$ [165]. Also, it has been shown that although STCD is not applicable to the continuous disorder-driven transition of the random-bond Ising model at zero temperature and field, it can be applied to the first-order field driven transitions of that model [166].

One important application of STCD is as a criterion to distinguish between second- and weak first-order transitions. Near a weak first-order transition there are two 'pseudo-critical points' $T^{**} < T_c < T^*$, which are close together in the weak first-order case, and become identical to T_c for second-order transitions. Using STCD with high (low) temperature initial conditions (i.e. $m_0 \simeq 0$ or $m_0 = 1$), the temperature T^* (T^{**})

can be determined. The difference $T^* - T^{**}$ is a measure of the strength of the transition, and it has been applied, among others, to the Potts model with $q = 5$ and $q = 7$ [167], the XY non-collinear magnets [120], and driven lattice gas (DLG) [168] (see section 4.1). Also, for the first-order irreversible phase transition of the ZGB model, the analysis of the STCD seems to agree with the spinodal point of the model [169]. The underlying idea is that T^* (T^{**}) is the upper (lower) spinodal point. At this point, the low (high) temperature phase becomes unstable, and in this sense it resembles the critical point of a second-order phase transition.

Based on these facts, it has recently been shown that STCD can be applied to the spinodal point in the fully connected Ising model [170] (in this mean-field-like model, the spinodal can be rigorously defined [171]). In this case, the extended free energy per particle, the spinodal fields h_{sp} and magnetizations m_{sp} were exactly calculated. Also, the complete set of (static) critical exponents associated with the divergences at the spinodal can be analytically derived. By taking the order parameter as $\Delta m = m - m_{sp}$, and assuming that the relationships of table 1 are valid by taking h as the control parameter instead of T, STCD has been successfully used to determine this spinodal. Fixing h at $h = h_{sp}$ and starting the simulation from the ordered initial condition ($\Delta m = 1$), the time series of the OP and its second moment (Δm and $\Delta m^{(2)}$) exhibit a power-law behaviour. Also, the static critical exponents can be correctly retrieved from the dynamic exponents using the equations of table 1.

The same study has been carried out for the nearest-neighbour q-state Potts model for different values of $q > 4$, where the transition is first order [170]. The transition temperature T_c and the lower spinodal magnetization m_{sp} are known exactly as $T_c(q)/J = 1/\ln(1+\sqrt{q})$ and $m_{sp} = 0$, respectively [172]. Figure 7 shows the dynamic behaviour of the magnetization and the corresponding second moment, starting from a completely disordered state for $q = 96$. One observes a clear power-law increase, spanning two decades in time, for $T = T_{sp}^{(-)} = (0.950 \pm 0.002)T_c$.

In the case of short-range interactions, STCD identifies pseudo-critical dynamic behaviour, which lasts for a finite time. This corresponds to the known fact that there is no true singularity in the spinodal zone [173]. The susceptibility and relaxation times of the metastable phase increase as one goes deeper into the metastable region, and if they are extrapolated with a power law, they seem to diverge at a point beyond the metastability limit [174, 175] called *pseudo-spinodal*. The pseudo-spinodal is very difficult to determine because one has to sample the metastable zone. Using two-time correlation functions and fluctuation–dissipation relations, one needs to ensure that the system is in (meta-)equilibrium and that no nucleation effects are present. Figure 8 shows the correlation time (τ_R), the specific heat (c_h), and the magnetic susceptibility (χ_T) computed in the stable and metastable regimes for the Potts model. All these quantities grow in a way compatible with a divergence at $T = T_{sp}^{(-)} = 0.950T_c$. Continuous lines are fits to a power law, while dashed lines (for c_h and χ_T) are corrections to the scaling used in order to include lower temperatures in the fit. So, the temperature $T_{sp}^{(-)}$ identified by STCD is equal to the pseudo-spinodal temperature.

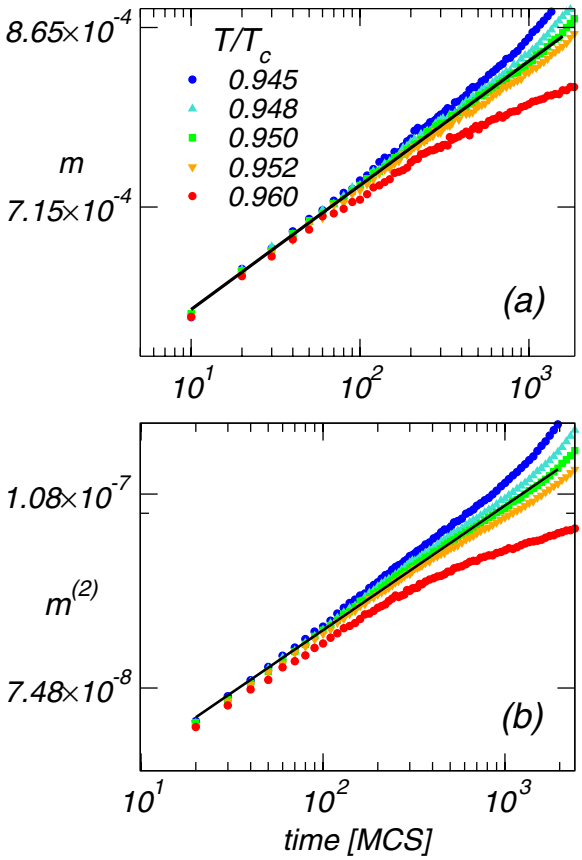

Figure 7. Short-time behaviour in a supercooled state at different temperatures for $q = 96$ and $L = 480$. Full lines are power-law fits for $T = 0.950T_c$. (*a*) Order parameter m; (*b*) second moment $m^{(2)}$. (Color online.)

The same behaviour is found for $q = 12$, 24, 48, 96 and 192. Figure 9 shows $(T_c - T_{sp}^{(-)})/T_c$ versus q, including the 'pseudo-critical' temperatures found in [167] with STCD analysis and for $q = 7$, 10 found in [175] by sampling stable states. The data are very well fitted by the logarithmic form $A\log^a(1+q-4)$ with $a = 3.10$, in qualitative agreement with the behaviour of the mean-field solutions.

Thus the STCD technique allows us to determine (pseudo)spinodals without need of equilibrium data, which is an essential requirement when using standard methods.

4. Non-equilibrium phase transitions

The formalism of statistical mechanics, as built upon the ideas of Boltzmann and Gibbs, must in principle be applied to systems in thermodynamic equilibrium. However, many interesting natural systems are found in out-of-equilibrium states. Non-equilibrium states display mass and energy fluxes, which can be generated by the boundary conditions (in space and/or time), by a time-dependent external field or both [176]. The non-equilibrium state in general cannot be characterized by the external parameters (temperature, potential gradients, etc) alone, and it depends on the whole history of the system. However, these parameters are enough to specify the state in the simplest case, namely when the fluxes are stationary. These states are called non-equilibrium steady states (NESSs).

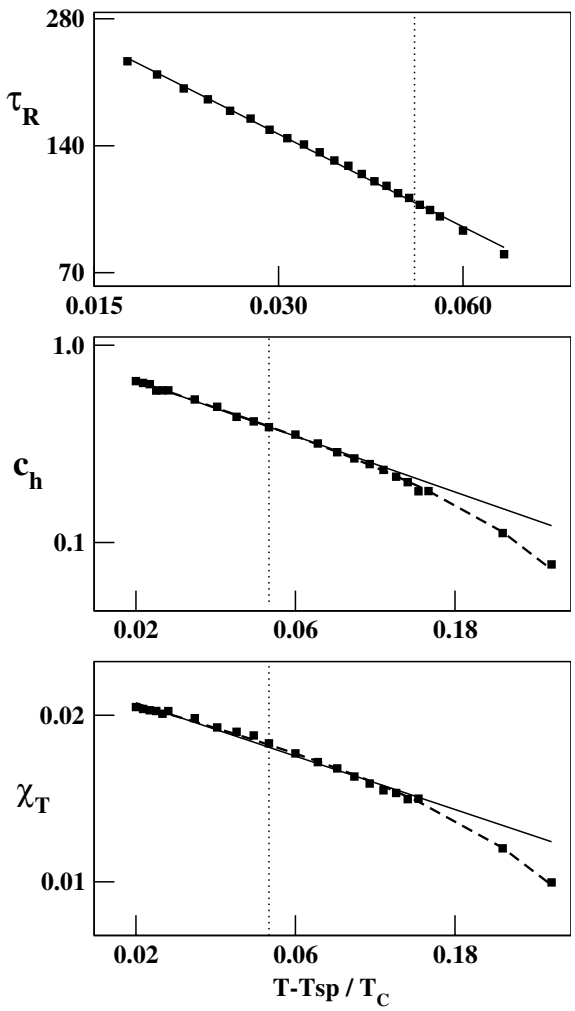

Figure 8. Relaxation time, specific heat and magnetic susceptibility as a function of $(T - T_{sp}^{(-)})/T_c$ in the metastable state for $q = 96$ and taking $T_{sp}/T_c = 0.950$. The continuous lines are power-law fits. The vertical dashed lines are $T = T_c$. The dashed lines are fits with a corrected power law [170].

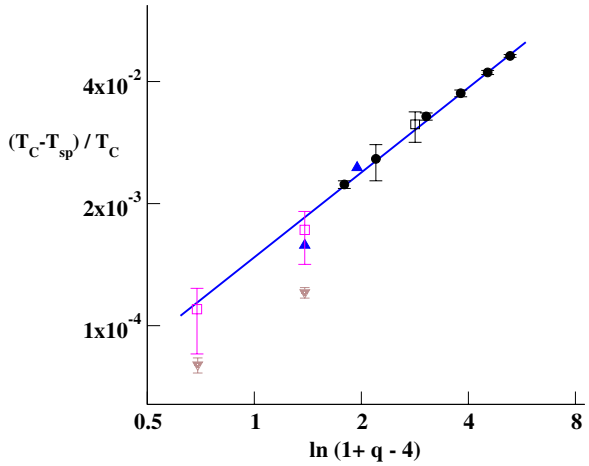

Figure 9. $(T_c - T_{sp}^{(-)})/T_c$ versus $\ln(1 + q - 4)$. For $q = 5, 7$ data were obtained using STCD analysis in [167], and for $q = 7, 10$ as pseudo-spinodals using stable states in [175]. The continuous line is a fit of the data with $A \ln^a(1 + q - 4)$ with $a \approx 3.10$. The triangles pointing up, down triangles, open dark squares and full circles are points obtained by Fernandez *et al* [175], Schülke and Zheng [167], Loscar *et al* [170] and Ozeki *et al* [165]. The open squares below $\ln(1 + q - 4) = 2$ are points obtained for this work. The new determination gives values for T_{sp} a little farther from the transition as compared with [167], and the difference is probably due to size effects (we used $L = 1000$ instead of $L = 560$).

Variation of the external parameters may destabilize the non-equilibrium state. These instabilities will cause a change of state, and can be followed by ordering phenomena analogous to those of equilibrium systems. These changes are called *non-equilibrium phase transitions* [177, 178].

There is no general theoretical framework yet to treat non-equilibrium phase transitions. Several approaches have been proposed, such as the search for exact solutions, mean-field theories, renormalization-group techniques, molecular dynamics and Monte Carlo simulations [8, 176]. In this context, the STCD technique has proved to be a very useful tool.

In this section, we review the results that have been obtained applying STCD to the driven lattice gas (section 4.1), the Vicsek model for collective displacement (section 4.2), and self-organized criticality (section 4.3).

4.1. The driven lattice gas

One of the simplest models that captures many essential features of non-equilibrium behaviour is the driven lattice gas (DLG), proposed by Katz *et al* [179]. It is an interacting system driven into NESSs by an external field. It exhibits remarkable properties, such as its non-Hamiltonian nature, the violation of the fluctuation–dissipation theorem, the occurrence of anisotropic critical behaviour [180], the existence of a unique relevant length scale in the anisotropic pattern formation at low temperatures and the consequent self-similarity in the system at different evolution times [181].

The 2D DLG is defined on a square lattice with rectangular geometry $(L_x \times L_y)$ and periodic boundary conditions. The degrees of freedom are the site occupation numbers $n_{i,j} = 0, 1$ $(i = 1, \ldots, L_x,\ j = 1, \ldots, L_y)$. With NN attractive interactions $(J > 0)$ and without field, the Hamiltonian corresponds to the Ising lattice gas,

$$H = -4J \sum_{\langle ij,i'j' \rangle} n_{i,j} n_{i',j'}, \tag{4.1}$$

where the sum runs over NN sites only and the dynamics are such that the density ρ_0 (fraction of sites with $n_{i,j} = 1$) is fixed. In MC simulations, a driving field E is introduced through a modified Metropolis probability,

$$p = \min[1, \exp(\Delta H - \eta E/k_B T)], \tag{4.2}$$

where ΔH is the change in H after the attempted move and η is -1, 0 or 1 for a particle hopping against, orthogonally or along the field, respectively.

At high T, the DLG exhibits a gas-like disordered state, but at low temperatures an anisotropic NESS emerges. This ordered phase is characterized by stripes of high and low density, aligned with the field axis. For $\rho_0 = 1/2$, the transition is continuous [180]. Extensive MC simulations have shown

that the critical temperature depends on the external field, and that it saturates for $E \to \infty$ at a value $T_c \simeq 1.41 T_O = 3.20$ ($T_O = 2.269\, J/k_B$ is the Onsager critical temperature of the 2D Ising model) [180]. The field generates a strong anisotropy and, as a result, a double set of critical exponents (longitudinal and transverse) is needed to account for both the critical dynamics and steady-state behaviour of the correlation lengths. For other values of the density, the transition is first-order [180].

4.1.1. The second-order case. The universality class of the second-order transition when $\rho_0 = 1/2$ has been the subject of a long-standing debate. In the first theoretical investigations, Janssen *et al* introduced a mesoscopic Langevin equation preserving mass conservation and the symmetries of the model (invariance under field reversal $E \to -E$ and particle–hole) and a term representing a current proportional to the external field. As usual, an uncorrelated white noise term represents the fast degrees of freedom. Using an expansion up to first order in $\epsilon = 5 - d$, it was found that the upper critical dimension is $d = 5$, and the static critical exponents for $d = 2$ in the $E \to \infty$ limit were calculated, obtaining $\beta = 1/2$ for the order parameter and $\nu_\parallel \approx 3/2$, $\nu_\perp \approx 1/2$ for the correlation length exponents in the parallel and perpendicular direction of the driving field, respectively. Thus it was concluded that the model belonged to a new universality [182–184]. The values found for these exponents are different from those found by Vallés and Marro in MC simulations, using the isotropic finite-size scaling theory to collapse the NESS data of the magnetization along the parallel direction [185]. These authors found $\beta \approx 1/3$. More recent simulations by Leung [186] instead found a good collapse of the data using anisotropic scaling expressions with the critical exponents of Janssen *et al* However, subsequent analysis of Leung's data by Achahbar and Marro [187] and Marro *et al* [188] showed that the data could also be collapsed using the critical exponents of Marro and co-workers in [185].

Due to this discrepancy, Garrido and co-workers [189] proposed an alternative theoretical treatment, starting from a master equation and obtaining a corresponding Langevin equation by performing a Kramers–Moyal expansion to second order in $\epsilon = 3 - d$. The main difference between this equation that of Janssen *et al* is that the term containing the external field vanishes in the $E \to \infty$ limit. The resulting equation was already known (it had been developed for a variant of the model called random driven lattice gas (RDLG), where the direction of the field changes randomly on each MC trial [190]). The critical exponents of the $d = 2$ DLG in the $E \to \infty$ limit were thus estimated with RG techniques as $\beta \approx 0.33$, $\nu_\parallel \approx 1.22$ and $\nu_\perp \approx 0.63$ [191–193], corresponding to the universality class of the RDLG. These results were later supported by the numerical results of Achahbar *et al*, who also employed anisotropic finite-size scaling theories to analyse the NESS data [194].

In the simulations summarized above, the NESS data are somewhat affected by the choice of the lattice aspect ratio $S = {L_y}^{\nu_\parallel/\nu_\perp}/L_x$. This is akin to assuming the ratio $\nu_\parallel/\nu_\perp$ is known *before* analysing the data, so the collapse will be biased towards one result. To avoid this bias, Albano *et al* studied the dynamical evolution of the DLG using STCD [195]. In this work, the early-time critical evolution of the model was investigated starting from two kinds of initial conditions: (a) fully disordered configuration (FDCs), which means that the system is initially placed in a thermal bath at $T \to \infty$, and (b) ground-state configuration (GSC) or the equilibrium $T = 0$ configuration, consisting of a single stripe at the centre of the lattice and directed along the field. The OP measures the density fluctuations along the field axis,

$$\mathrm{OP} = (RL_y)^{-1} \sum_{i=1}^{L_y} |P(i) - \rho_0|, \tag{4.3}$$

where $L_{y(x)}$ is the lattice size in the perpendicular (parallel) direction to the applied field, $P(i) = (L_x)^{-1} \sum_{i=1}^{L_x} \eta_{ij}$ is the perpendicular density profile, ρ_0 is the particle density and $R = 2\rho_0(1 - \rho_0)$ is a normalization constant.

Assuming an anisotropic scaling, the authors proposed the following ansätze for the short-time evolution of $\mathrm{OP}(t)$: starting the system from FDCs,

$$\mathrm{OP}(t, \tau, L_x) = b^{-\beta/\nu_\parallel} \mathrm{OP}^*(b^{-z_\parallel} t, b^{1/\nu_\parallel} \tau, b^{-1} L_x), \tag{4.4}$$

and starting from GSC,

$$\mathrm{OP}(t, \tau) = b^{-\beta/\nu_\perp}\, \widetilde{\mathrm{OP}}(b^{-z_\parallel} t, b^{1/\nu_\perp} \tau), \tag{4.5}$$

where $\tau = T - T_c/T_c$, OP^* and $\widetilde{\mathrm{OP}}$ are scaling functions, b is a spatial rescaling factor, β is the critical exponent of the OP, $\nu_{\parallel(\perp)}$ is the longitudinal (transverse) critical exponent of the correlation length and $z_\parallel$ is the corresponding dynamic critical exponent. By setting $b \sim t^{1/z_\parallel}$ in both equations, the time evolution of $\mathrm{OP}(t)$ is obtained as

$$\mathrm{OP}(t, \tau, L_x) \propto L_x^{-1/2} t^{c_1} \mathrm{OP}^{**}(t^{1/\nu_\parallel z_\parallel} \tau) \qquad \text{(FDC)}, \tag{4.6}$$

$$\mathrm{OP}(t, \tau) \propto t^{-c_3}\, \widetilde{\widetilde{\mathrm{OP}}}(1, t^{1/\nu_\perp z_\parallel} \tau) \qquad \text{(GSC)}, \tag{4.7}$$

where $c_1 = (1 - 2\beta/\nu_\parallel)/2z_\parallel$ and $c_3 = \beta/\nu_\perp z_\parallel$. Also, in (4.6), $L_x^{-1/2}$ is the initial amplitude of OP that is originated from the construction of the FDC configurations [195], and its scaling form was conjectured from the empirical data. As c_1 and c_3 are not enough to obtain the complete set of exponents, the calculation of the derivative of $\ln \mathrm{OP}(t)$ (or $\mathrm{OP}(t)$) with respect to τ (at the critical point) is needed in the FDC (GSC) case,

$$\partial_\tau \ln \mathrm{OP}(t, \tau)|_{\tau=0} \propto t^{c_2} \qquad \text{(FDC)}, \tag{4.8}$$

$$\partial_\tau \mathrm{OP}(t) \propto t^{c_4} \qquad \text{(GSC)}, \tag{4.9}$$

where $c_2 = 1/\nu_\parallel z_\parallel$ and $c_4 = (1 - \beta)/\nu_\perp z_\parallel$. In this way, all critical exponents, except $z_\perp$, can be computed since all expressions above only take into account the critical dynamic behaviour of the parallel correlation length through the exponent $z_\parallel$. In fact, as shown numerically in [196], critical correlations along the driving field axis are dynamically dominant over the transverse correlations *in the short-time scale*, regardless of the initial condition. This fact contradicts the idea that the longitudinal (transverse) correlations must develop first when the system is started in the FDC (GSC)

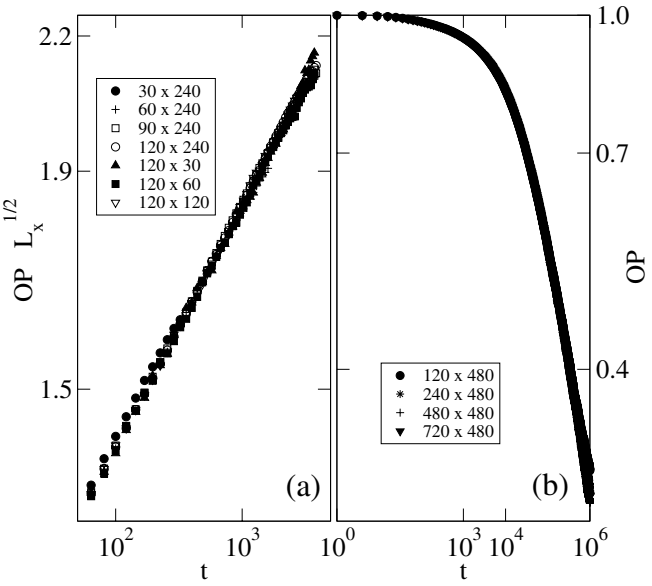

Figure 10. Double log plots of the time evolution of the order parameter OP(t) at the critical temperature for the DLG with FDC (a) and GSC (b) initial conditions. The system sizes employed are indicated in the legend with the notation $L_x \times L_y$. Note that in the FDC case all curves can be collapsed by accounting for the initial ordering using equation (4.6).

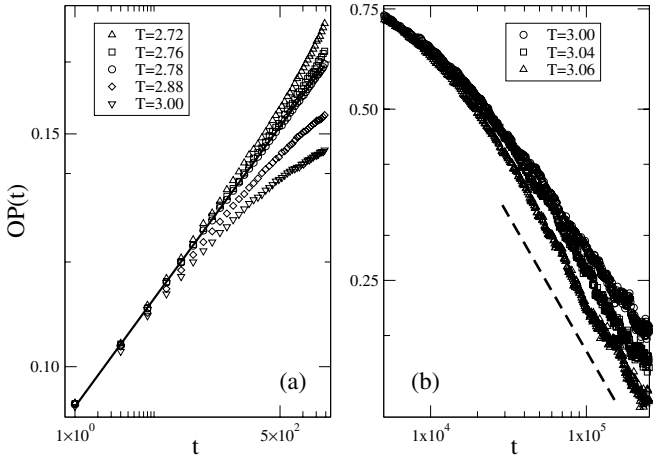

Figure 11. Log–log plot of the short-time evolution of OP(t) for the DLG with $\rho_0 = 0.25$. (a) Starting from FDCs, a very good straight line can be fitted at $T = T^{**} = 2.78$, while upward (downward) deviations can also be observed for $T < T^{**}$ ($T > T^{**}$). The data corresponding to $T = 2.78$ can be fitted by a straight line, suggesting that this temperature is the lower bound of ΔT for this density. (b) Log–log plot of the long-time evolution of OP(t) versus t when the system starts from a GSC configuration. The dashed line indicates the zone where the pseudo-power law is observed. The pseudo-critical temperature is $T^* = 3.04$.

Table 11. Critical temperatures and exponents of the DLG and RDLG models, obtained through STCD, and those calculated by the theoretical approaches summarized in the text.

Model	T_c	β	$\nu_\parallel$	$\nu_\perp$
DLG	3.200(10)	0.330(30)	1.221(40)	0.644(40)
RDLG	3.160(20)	0.311(30)	1.168(40)	0.671(40)
Janssen's equation [182–184]	—	1/2	$\simeq$3/2	$\simeq$1/2
Garrido's equation [189]	—	$\simeq$0.33	$\simeq$1.22	$\simeq$0.63

initial conditions, in order to uniquely describe the long-time behaviour of OP(t) [197].

When T is tuned to the critical temperature, OP(t) follows a power law (figure 10). Critical exponents obtained from exponents c_i are in good agreement with the values of the field-theoretical description of Garrido *et al* [191–193]. Unlike previous studies under NESS conditions [186, 194], the data are not biased by assumptions about lattice shape [179, 180], which must be fixed in stationary simulations due to the anisotropy of the system.

In the same work, the RDLG was studied [195], finding the same values for the exponents and thus concluding that DLG and RDLG belong to the same universality class, as predicted by Garrido *et al*. All of the obtained results are summarized in table 11.

4.1.2. The first-order case. For $\rho_0 < 1/2$, STCD gives upper and lower bounds, T^{**} and T^*, for the coexistence point T_{coex} (similarly to the equilibrium first-order case; see section 3.6). The interval $\Delta T = T^* - T^{**}$ is a measure of the 'strength' of the transition [167]. In this model, ΔT is expected to decrease when ρ_0 increases, vanishing at $\rho_0 = 1/2$, where $T^{**} = T^* = T_c$. Using the order parameter defined above (section 4.1), Saracco and Albano [168] determined the interval ΔT for several values of ρ_0 (see figure 11).

Collecting all of the intervals ΔT corresponding to different densities, plus the data for the critical point, it is possible to draw the phase diagram, T_c versus ρ_0, for the DLG (figure 12). ΔT (grey area) decreases as $\rho_0 \to 1/2$, indicating that the first-order transition is progressively weaker, eventually becoming second-order at $\rho_0 = 1/2$. The coexistence points T_{coex} were found by letting the system reach NESS states [168] (also shown in figure 12). As expected, the points obtained from NESS lie within the interval ΔT for each investigated density, as in equilibrium systems (section 3.6).

4.2. Dynamics of collective displacement of self-driven individuals

A fascinating feature of groups of interacting agents moving together is the (far-from-equilibrium) phenomenon of ordered collective motion. It can be found in nature at almost every spatial scale and with quite diverse types of individuals: herds of quadrupeds [198, 199], human crowds [199], bird flocks [200], fish schools [201] or even as unicellular organisms [202, 203] or individual cells within a larger organism [204].

The physicist's approach to the problem of collective motion is to try to identify the universal features of the phenomenon, rather than attempt a detailed case-by-case description. Thus one looks for the simplest model displaying the universal features. In the problem of collective motion, the archetypical model is that proposed by Vicsek *et al* [205]. The Vicsek model (VM) considers N point-like individuals in d-dimensions, with (off-lattice) positions $\vec{x}_i$ and velocities $\vec{v}_i$

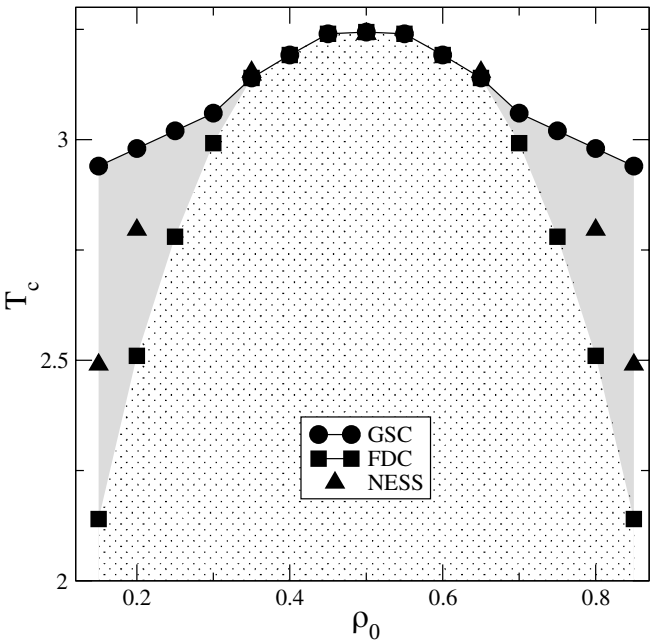

Figure 12. Phase diagram for the DLG showing the dependence of T_c on ρ_0. The points labelled by triangles are obtained by means of NESS measurements (NESS transition points), and using particle–hole symmetry. The lower and upper bounds obtained by means of the STCD analysis are also displayed. The squares are the lower bounds obtained when the system is initiated taking FDCs, while the circles are the upper bounds corresponding to those systems started with GSCs. The grey area indicates the decrease in the T interval Δ.

moving in direction θ_i ($i = 1, 2 \ldots N$). To simply account for the self-propelled nature of the motion, the magnitude of the velocity is fixed at v_0. Individuals interact locally by trying to align their directions of motion with those of their neighbours, in the presence of some noise. In practice, this is implemented by setting, at each time step, the direction of a given individual to the average direction of individuals located within a sphere of radius R_0, plus some random noise,

$$\theta_i^{t+1} = \arg\left[\sum_{j\in\mathcal{S}_i} e^{i\theta_j^t}\right] + \xi_i^t. \tag{4.10}$$

where $\mathcal{S}_i$ is the sphere centred on the individual i, and the noise ξ is uniformly distributed in the interval $[-\eta\pi, \eta\pi]$. The positions are updated according to

$$\vec{x}_i(t + \Delta t) = \vec{x}_i(t) + \vec{v}_i(t)\Delta t. \tag{4.11}$$

The OP describing the collective behaviour is the normalized average velocity,

$$\varphi \equiv \frac{1}{N v_0}\left|\sum \vec{v}_i\right|. \tag{4.12}$$

For individuals moving almost randomly, one has $\varphi \sim 0$, whereas when all individuals tend to move in the same direction, $\varphi \to 1$.

Although the VM is a far-from-equilibrium system obeying dynamics quite different from those of standard ferromagnetic models (Ising or XY), it behaves similarly in the sense that in both there is a tendency for the spin (here velocity) to align with its neighbours (see section 4.10). The noise amplitude η is roughly analogous to the temperature. In this sense, it is not surprising that the VM exhibits order–disorder transitions. In the low velocity regime ($v\Delta t \ll 1$), individuals tend to order when the noise is decreased below a critical value $\eta_c(\rho, v_0)$ (ρ is the number density). The critical point and exponents of the second-order transition have been evaluated by both standard finite-size scaling and STCD (see table 12). The critical exponents satisfy the hyperscaling relation (for $d = 2$),

$$d - 2\frac{\beta}{\nu} - \frac{\gamma}{\nu} = 2 - 2\cdot 0.275 - 1.45 = 0.00(3). \tag{4.13}$$

To obtain reliable critical exponents from relaxational dynamics, one has to start the simulations from 'naturally' ordered configurations, i.e. configurations having the proper correlations generated by the dynamics of the VM in the $\eta \to 0$ limit [206]. Figure 13 (right-hand side) shows plots of φ versus t for different N with constant $\rho = N/L^2$. By setting $b = L$ in equation (2.9) at criticality, one has

$$\varphi(t, L) \sim L^{-\beta/\nu}\widetilde{\widetilde{\varphi}}(t/L^z), \tag{4.14}$$

where the factor $L^{-\beta/\nu}$ simply reflects the scaling behaviour of the OP for the long-time stationary regime. More interestingly, the argument of the scaling function $\widetilde{\widetilde{\varphi}}$ suggests that log–log plots of the OP versus the rescaled time t/L^z should collapse in the short-time regime. This is observed in figure 13 (left-hand side), which confirms the validity of the dynamic scaling anzatz.

It has been argued that the VM can be considered a non-Hamiltonian version of the XY model [205], since it has many symmetries in common with the former (the main difference, of course, being that the spins of the VM move in continuous space). However, the critical behaviour of VM, as characterized by dynamic measurements, is quite different from that of XY. In fact, Bray *et al* [207] have shown that the dynamic critical scaling for the case of the 2D-XY model breaks down because the rate of approach to equilibrium depends on the initial condition ($\xi(t) \sim t^{1/2}$ ($z = 2$) if the initial state is ordered and $\xi(t) \sim [t/\ln(t)]^{1/2}$ when the initial state is disordered). In contrast, the dynamic exponent of the VM ($z \cong 1.28(3)$) is independent of the initial state [206].

Very recently, Wood *et al* [208] reported that a non-equilibrium lattice model for stochastic coupled oscillators, which can be described with the same order parameter as the VM, exhibits dimensionality dependent phase transitions (again the main difference is that oscillators are in fixed positions). The lower critical dimension for the observation of long-range order is $d = 2$, and in $d = 3$ the model undergoes a continuous phase transition in the equilibrium XY model universality class [208]. The universality classes of other far-from-equilibrium systems with continuous phase transitions have extensively been reviewed by several authors [209–212]. After a careful analysis [206], it can be concluded that the VM may define its own universality since its set of exponents is quite different from those characteristics of other well-established universality classes. The above findings suggest that the coupling between orientation and displacement is essential for establishing long-range order in $d = 2$.

Table 12. Exponents of the VM in $d = 2$ as obtained by stationary measurements (S), relaxation dynamics from ordered states (RD), and dynamic measurements starting from disordered configurations (DC) [206].

	$\frac{\gamma}{\nu}$	z	$\frac{\gamma}{\nu z}$	$\frac{\beta}{\nu z}$	$\frac{1}{\nu z}$	β	ν	γ	$\frac{\beta}{\nu}$
S	1.45(2)	—	—	—	—	0.45(3)	1.6(3)	2.3(4)	0.275(5)
RD	—	1.27(2)	—	0.25(2)	0.6(1)	0.42(4)	1.3(3)	—	0.32(3)
DC	—	—	1.12(3)	—	—	—	—	—	—
DC + RD	1.43(3)	—	—	—	—	—	—	1.87(4)	—
S + RD	—	—	1.13(3)	0.22(2)	0.5(1)	0.45(7)	—	1.89(4)	—
S + DC	—	1.29(3)	—	—	0.5(1)	—	—	—	—

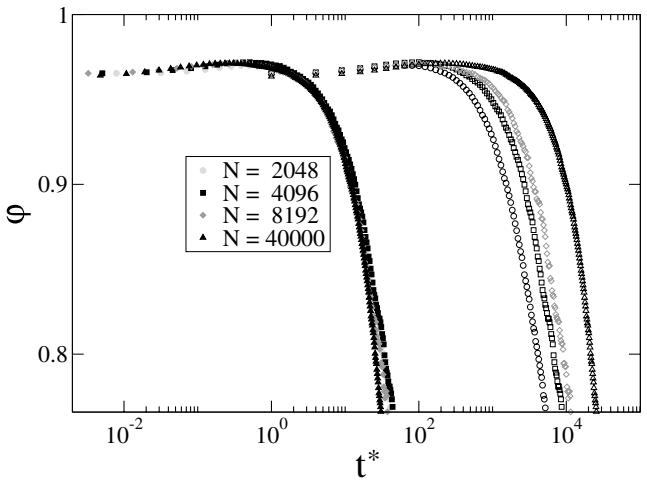

Figure 13. Log–log plots of the relaxation of the order parameter versus t^*. Data obtained by starting with naturally ordered configurations that are subsequently quenched to the critical point. Here, $t^* = t$ corresponds to the raw data (right-hand side), while $t^* = t/L^z$ corresponds to the rescaled horizontal axis (left-hand side) according to equation (4.14). Data obtained using four samples of different sizes.

4.3. Short-time behaviour of self-organized criticality (SOC) models

The term self-organized criticality (SOC) was introduced by Bak *et al* [213, 214] to describe complex systems capable of evolving towards a critical state without the need of tuning a control parameter. In contrast, the cases of critical behaviour discussed so far critical points are reached by tuning parameters such as field, temperature and pressure. SOC has attracted huge attention due to its ubiquity in a great variety of systems in the fields of biology (evolutionary models), geology (earthquakes), physics (flick noise), zoology (prey-predators and herds), chemistry (chemical reactions), social sciences (collective behaviour of individuals), ecology (forest fire), neurology (neural networks), etc. [215, 216].

It was recently shown [217] that the dynamic approach to the SOC regime when starting far from criticality can be described with a generalization of the dynamic scaling described in section 2. These concepts were applied to the evolutionary Bak-Sneppen (BS) model [218–222], and subsequently to John Conway's game of life (GoL) [223], showing in both cases that the approach to the SOC state is in fact critical [217, 224], and that its study allows the evaluation of critical exponents in excellent agreement with independent measurements performed within the SOC regime.

The BS model attempts to simulate the evolution of life through individual mutations and their relation in the food chain [218–222]. Each site of a d-dimensional array of side L represents a species whose fitness is given by a random number f drawn from a distribution $P(f)$ uniform in the range [0, 1]. The system evolves according to the following rules: (1) the site with the smallest fitness is chosen. (2) A new fitness is assigned to that site (a random number taken from P). This rule is based on the Darwinian survival principle that the species with less fitness are replaced or mutated. (3) At the same time, the fitness of the NN sites is changed. This rule simulates the impact of the mutation on the environment. The BS model exhibits a stationary (SOC) state where the density ρ of sites with fitness below a critical value is negligible ($f < f_c$, with $f_c = 0.66\,702(3)$), but it is uniform above f_c [222]. Within the SOC state, the BS model exhibits scale-free evolutionary avalanches and a punctuated equilibrium [218, 222].

To analyse the STCD of the BS, one assumes that each lattice site can be in one of two states σ_i: occupied ($\sigma_i = 1$) when its fitness is below f_c, or empty ($\sigma_i = 0$) when its fitness is above f_c. Then, since the Ising magnetization goes to zero at the critical temperature and in the BS the density of occupied sites ρ vanishes when the SOC state is reached [222], one proposes a scaling ansatz for the density. In the limit $L \to \infty$, it has been proposed that (see also equation (2.1))

$$\rho(t, \rho_0) = b^{-\aleph}\rho(b^{-z}t, b^{x_0}\rho_0), \tag{4.15}$$

where ρ_0 is the initial density, z is the dynamic exponent, x_0 is the exponent of the rescaling of ρ_0 and b is a scaling variable.

Figure 14 shows the evolution of the density $\rho(t, \rho_0)$ for different values of ρ_0. Three regimes can be distinguished, as follows. (i) A *short-time regime* ($0 < t < t_{max} \approx 10^3$), which holds for low initial densities $\rho_0 < 0.1$, where the density exhibits an initial increase. The value of the 'effective' exponent slightly depends on ρ_0; an extrapolation gives $\theta = 0.12(2)$ for $\rho_0 \to 0$. (ii) An *intermediate-time regime* ($t_{max} < t < t_{stat} \approx 10^6$), where the density decreases also following a power law with exponent $\delta = 0.47(2)$. (iii) A *long-time regime* ($t_{stat} < t$), where the system arrives at a stationary state with a constant average density ρ_{stat}. By means of scaling arguments, it can in addition be shown that $t_{max} \sim \rho_0^{1-D}$, where $D = 2.43(1)$ [222] is the *mass dimension* exponent.

The *time-scaling behaviour* of the density can be obtained from (4.15) by setting $b = t^{1/z}$, which yields

$$\rho(t, \rho_0) = t^{-\aleph/z}\Phi(t^{x_0/z}\rho_0), \tag{4.16}$$

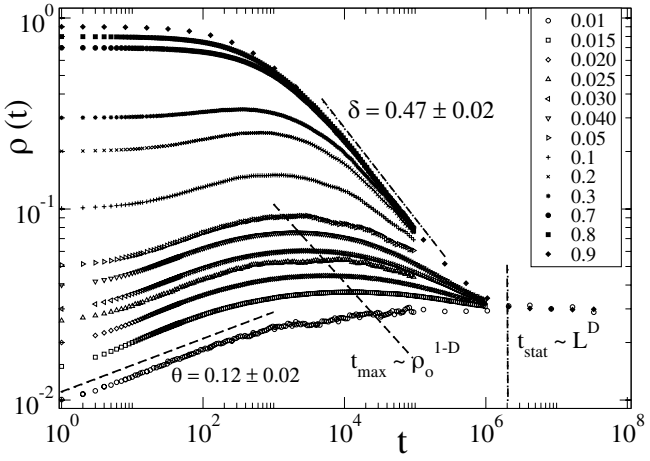

Figure 14. Time evolution of average density for several values of initial density ρ_0 as given. The three different regimes that can be observed are discussed in detail in the text.

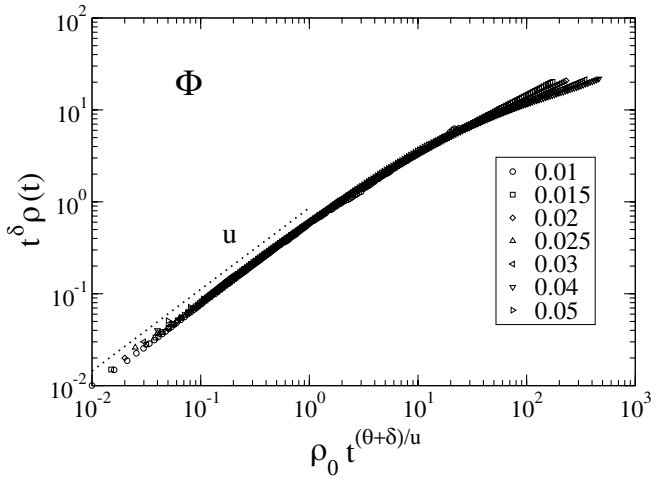

Figure 15. Scaling plot of the data shown in figure 14 obtained by using equation (4.19) for the time-scaling behaviour. The dotted line—slightly shifted up for the sake of clarity—with slope $u = 0.89$ corresponds to the best fit of the data obtained for the lowest density.

where Φ is a scaling function. For $\rho_0 \to 1$ and within the intermediate-time regime, $\rho(t)$ becomes independent of ρ_0 (see figure 14). Thus, assuming $x_0/z > 0$, one has $\Phi(t^{x_0/z}\rho_0 \gg 1) = \text{const}$, which holds for $t \gg t_{\max} \propto \rho_0^{-z/x_0} \propto \rho_o^{1-D}$. Then $t_{\max}$ sets the time scale for the initial increase in the density, as shown in figure 14. For the sake of comparison, it can be noted that in magnetic systems the time scale of the initial increase in the magnetization is set by $t_{\max} \propto m_o^{-z/x_0}$ (see equations (2.3) and (2.4)), where $m_0 \to 0$. Also, ρ should decrease according to

$$\rho(t) \sim t^{-\delta}, \tag{4.17}$$

with $\delta \equiv \aleph/z = 0.47(2)$. On the other hand, for $\rho_0 \to 0$ and within the short-time regime ($t \ll t_{\max}$, $t \to 0$), the dependence of Φ on the initial density becomes relevant, thus one has $\Phi(x) \sim x^u$. Hence, by replacing in (4.16), one has

$$\rho(t, \rho_0) = \rho_0^u t^\theta, \tag{4.18}$$

where $\theta = -\delta + ux_0/z$. So, $\theta = 0.12(2)$ is the exponent that describes the initial increase in the density within the critical STCD regime of the BS.

On the other hand, by replacing $\frac{x_0}{z} = \frac{\theta+\delta}{u}$ in equation (4.16), one obtains [217]

$$\rho(t, \rho_0) = t^{-\delta}\Phi(\rho_0 t^{\frac{\theta+\delta}{u}}). \tag{4.19}$$

The shape of the scaling function Φ is shown in figure 15. The excellent collapse of the data shown in figure 14 strongly supports the scaling hypothesis and the calculated exponents. In fact, the best fit of the data obtained, for $\rho_0 \to 0$, gives $u = 0.89(3)$ (see dotted line covering two decades in figure 15), which is in agreement with an independent determination that yields $u = 0.87(3)$ [217].

Further information on the dynamic evolution towards the SOC regime can be obtained by computing the *time autocorrelation* of the state of the site, $A(t, t_0)$ (averaged over all sites), which is expected to decay according to a power law (see table 1),

$$A(t_0, t) = \langle\sigma_i(t_0)\sigma_i(t)\rangle - \langle\sigma_i(t_0)\rangle\langle\sigma_i(t)\rangle \sim t^{-\lambda}, \tag{4.20}$$

where $\sigma_i(t) = 1, 0$ is the state of the site at time t, and $\lambda = d/z - \theta$. Extensive simulations have yielded $\lambda = 0.35(2)$, which combined with the value $\theta = 0.12(2)$ gives for the dynamic exponent $z = 2.13(5)$. Also, from $1 - \theta = z/D$ one obtains $D = 2.42(5)$ [217]. These figures are in agreement with those obtained within the SOC regime [222], i.e. $z = 2.1(5)$ and $D = 2.43(1)$.

The STCD scaling approach to SOC has also been applied to the GoL. This is a cellular automaton that, by means of a few local rules, simulates the dynamic behaviour of a society of living individuals including birth, death, survival and competition. GoL is implemented in $d = 2$ dimensions. Simulations of the approach to the SOC state yield [224] $\delta \equiv \aleph/z = 0.28(2)$, $\theta = 0.11(2)$, $u = 1.10(5)$, $\lambda = 0.35(5)$ and $z = 2.10(5)$. Again, all relevant critical exponents can be determined by studying the dynamic behaviour of the model.

In summary, the dynamic approach to SOC is critical, and it is ruled by the dynamic exponent z, the stationary exponents and the exponent θ that describes the initial increase in the density. The criticality observed in the approach to the SOC state not only addresses new and challenging theoretical aspects of SOC behaviour but is also of practical importance for the determination of the relevant exponents.

5. Conclusions and perspectives

In this review, we provide and discuss extensive evidence showing that the Monte Carlo method provides a useful and versatile tool for the practical implementation of the dynamic theory of critical phenomena. By performing dynamic simulations with carefully selected initial conditions (in most cases, ground state and full disorder), one can determine the critical value of the control parameter and the static and dynamic exponents. Static exponents are in full agreement with independent determinations obtained by means of equilibrium configurations. On the other hand, in order to describe the initial slip of the order parameter, an additional (dynamic) exponent is needed.

Dynamic Monte Carlo simulations are not restricted to the study of equilibrium phase transitions, where an underlying and well-established theory (the renormalization group) exists, but they can be used with a wide variety of systems, including far-from-equilibrium critical phenomena and irreversible phase transitions. Also, they have allowed one to gain insight into the properties of spinodal points in first-order phase transitions. Recently, it was also shown that the dynamic evolution towards the self-organized critical (SOC) regime is also critical, in the sense that it can be described by a set of critical exponents that also characterize the SOC state. Of course, all of these numerical results go one step beyond the original theoretical predictions and pose a formidable challenge that defines an interesting opportunity for further research. We expect that in the coming years the Monte Carlo method will provide new and interesting evidence on the dynamic critical behaviour of other non-conventional systems, such as those of interest in the fields of biology, social dynamics and complex systems in general.

Acknowledgments

We acknowledge financial support from Consejo Nacional de Investigaciones Científicas y Técnicas, Agencia Nacional de Promoción Científica y Tecnológica and Universidad Nacional de La Plata (Argentina).

References

[1] Janssen H K, Schaub B and Schmittmann B 1989 New universal short-time scaling behaviour of critical relaxation processes *Z. Phys.* B **73** 539–49
[2] Zheng B 1998 Monte Carlo simulations of short-time critical dynamics *Int. J. Mod. Phys.* B **12** 1419–84
[3] Calabrese P and Gambassi A 2005 Ageing properties of critical systems *J. Phys. A: Math. Gen.* **38** 133–93
[4] Godreche C and Luck J M 2002 Nonequilibrium critical dynamics of ferromagnetic spin systems *J. Phys.: Condens. Matter* **14** 1589
[5] Hohenberg P C and Halperin B I 1977 Theory of dynamic critical phenomena *Rev. Mod. Phys.* **49** 435–79
[6] Calabrese P, Gambassi A and Krzakala F 2006 Critical ageing of Ising ferromagnets relaxing from an ordered state *J. Stat. Mech.: Theory Exp.* **2006** P06016
[7] Calabrese P and Gambassi A 2007 Slow dynamics in critical ferromagnetic vector models relaxing from a magnetized initial state *J. Stat. Mech.: Theory Exp.* **2007** P01001
[8] Cardy J 1996 *Scaling and Renormalization in Statistical Physics* (Cambridge: Cambridge University Press)
[9] Janssen H K 1992 On the renormalized field theory of nonlinear critical relaxation *From Dynamical Chaos to Diffusion, From Phase Transitions to Chaos* (Singapore: World Scientific) pp 68–91
[10] Huse D A 1989 Remanent magnetization decay at the spin-glass critical point: a new dynamic critical exponent for nonequilibrium autocorrelations *Phys. Rev.* B **40** 304–8
[11] Schülke L and Zheng B 1996 Determination of the critical point and exponentes from short-time dynamics *Phys. Lett.* A **215** 81–5
[12] Fernandes H A, Arashiro E, Drugowich de Felício J R and Caparica A A 2006 An alternative order parameter for the 4-state Potts model *Physica* A **366** 255–64
[13] Jaster A, Mainville J, Schülke L and Zheng B 1999 Short-time critical dynamics of the three-dimensional Ising model *J. Phys. A: Math. Gen.* **32** 1395–406
[14] Tome T and de Oliveira M J 1998 Short-time dynamics of critical nonequilibrium spin model *Phys. Rev.* E **58** 4242–5
[15] Santos M and Figueiredo W 2001 Critical dynamics of the Baxter Wu model *Phys. Rev.* E **63** 042101
[16] Bab M A, Fabricius G and Albano E V 2006 Discrete scale invariance effects in the nonequilibrium critical behavior of the Ising magnet on a fractal substrate *Phys. Rev.* E **74** 041123
[17] Bab M A, Fabricius G, and Albano E V 2009 Critical exponents of the Ising model on low-dimensional fractal media *Physica* A **388** 370–8
[18] Arashiro E and Drugowich de Felício J R 2003 Short-time critical dynamics of the Baxter–Wu model *Phys. Rev.* E **67** 046123
[19] Fernandes H A, da Silva R and Drugowich de Felício J R 2006 Short-time critical and coarsening dynamics of the classical three-dimensional Heisenberg model *J. Stat. Mech.: Theory Exp.* **10** P10002
[20] Baxter R J 1982 *Exactly Solved Models in Statistical Mechanics* (New York: Academic)
[21] Okano K, Schülke L and Zheng B 1998 Dynamic $SU(2)$ lattice gauge theory at finite temperature *Phys. Rev.* D **57** 1411–14
[22] Santos M 2000 Short-time dynamics for the transverse Ising model *Phys. Rev.* E **61** 7204–7
[23] Grinstein G, Jayaprakash C and He Y 1985 Statistical mechanics of probabilistic cellular automata *Phys. Rev. Lett.* **55** 2527–30
[24] de Oliveira M J 1992 Isotropic majority-vote model on a square lattice *J. Stat. Phys.* **66** 273–81
[25] Teper M 1993 The finite-temperature phase transition of $SU(2)$ gauge fields in 2 + 1 dimensions *Phys. Lett.* B **313** 417–24
[26] Zheng B 2000 Monte Carlo simulations and numerical solutions of short-time critical dynamics *Physica* A **283** 80–5
[27] Wang F G and Hu C K 1997 Universality in dynamic critical phenomena *Phys. Rev.* E **56** 2310–13
[28] Okano K, Schülke L, Yamagishi K and Zheng B 1997 Universality and scaling in short-time critical dynamics *Nucl. Phys.* B **485** 727–46
[29] Nightingale M P and Blöte H W J 2000 Monte Carlo computation of correlation times of independent relaxation modes at criticality *Phys. Rev.* B **62** 1089–101
[30] da Silva R, Alves N A and Drugowich de Felício J R 2002 Mixed initial conditions to estimate the dynamic critical exponent in short-time Monte Carlo simulation *Phys. Lett.* A **298** 325–9
[31] Falk U, Furrer A, Güdel H U and Kjems J K 1986 Three-spin interaction in $CsMn_{0.28}Mg_{0.72}Br_3$ *Phys. Rev. Lett.* **56** 1956–9
[32] Turban L 1982 Self-dual Ising chain in a transverse field with multispin interactions *J. Phys. C: Solid State Phys.* **15** L65–8
[33] Wood D W and Griffiths H P 1972 A self dual relation for an Ising model with triplet interactions *J. Phys. C: Solid State Phys.* **5** L253–5
[34] Baxter R J and Wu F Y 1973 Exact solution of an Ising model with three-spin interactions on a triangular lattice *Phys. Rev. Lett.* **31** 1294–7
[35] Simões C S and Drugowich de Felício J R 2001 Dynamic critical exponents of the Ising model with multispin interactions *Mod. Phys. Lett.* B **15** 487–96
[36] Alcaraz F C and Barder M N 1987 Conformal invariance and the critical behavior of a quantum spin Hamiltonian with three-spin coupling *J. Phys. A: Math. Gen.* **20** 179–88

[37] Arashiro E, Fernandes H A and Drugowich de Felicio J R 2009 A comparative study of the dynamic critical behavior of four-state Potts-like models *Physica* A **388** 4379

[38] Majumdar S N, Bray A J, Cornell S J and Sire C 1996 Global persistence exponent for nonequilibrium critical dynamics *Phys. Rev. Lett.* **77** 3704–7

[39] Chen K, Ferrenberg A M and Landau D P 1993 Static critical behavior of three-dimensional classical Heisenberg models: a high-resolution Monte Carlo study *Phys. Rev.* B **48** 3249–56

[40] Zelli M, Boese K and Southern B W 2007 Short-time dynamic study of Heisenberg noncollinear magnet *Phys. Rev.* B **76** 224407

[41] Fernandes H A, Drugowich de Felício J R and Caparica A A 2005 Short-time behavior of a classical ferromagnet with double-exchange interaction *Phys. Rev.* B **72** 054434

[42] Caparica A A, Bunker A and Landau D P 2000 Classical ferromagnet with double-exchange interaction: high-resolution Monte Carlo simulations *Phys. Rev.* B **62** 9458–62

[43] Környei L, Pleimling M and Iglói F 2008 Nonequilibrium critical dynamics of the two-dimensional Ising model quenched from a correlated initial state *Phys. Rev.* E **77** 011127

[44] Chen Y, Guo S H, Li Z B, Marculescu S and Schuelke L 2000 Short-time critical bahaviour of the Ginzburg-Landau model with long-range interaction *Eur. Phys. J.* B **18** 289–96

[45] Luijten E and Blöte H W J 1997 Classical critical behavior of spin models with long-range interactions *Phys. Rev.* B **56** 8945–58

[46] Bergersen B and Rácz Z 1991 Dynamical generation of long-range interactions: random Levy flights in the kinetic Ising and spherical models *Phys. Rev. Lett.* **67** 3047–50

[47] Chen Y 2002 Short-time dynamics of a random Ising model with long-range interaction *Phys. Rev.* E **66** 037104

[48] Chen Y, Guo S, Li Z and Ye A 2000 Short-time behavior of the kinetic spherical model with long-ranged interactions *Eur. Phys. J.* B **15** 97–104

[49] Baumann F, Dutta S B and Henkel M 2007 Kinetics of the long-range spherical model *J. Phys. A: Math. Gen.* **40** 7389–409

[50] Uzelac K, Glumac Z and Barisic Z 2008 Short-time dynamics in the 1d long-range potts model *Eur. Phys. J.* B **63** 101–8

[51] Rodríguez D E, Bab M A and Albano E V 2009 Study of the nonequilibrium quenching and annealing dynamics for the long-range Ising model, arXiv:0908.1518v1

[52] Aizenman M, Chayes J T, Chayes L and Newman C M 1988 Discontinuity of the magnetization in one-dimensional 1/xy2 Ising and Potts models *J. Stat. Phys.* **50** 1–40

[53] Reynal S and Diep H T 2004 Reecamination of the long-renge pottsmodel: a multicanonical approach *Phys. Rev.* E **69** 026109

[54] Cardy J L 1981 One-dimensional models with l/r^2 interactions *J. Phys. A: Math. Gen.* **14** 1407–15

[55] Binder K and Luijten E 2001 Monte Carlo tests of renormalization-group predictions for critical phenomena in Ising models *Phys. Rep.* **344** 179–253

[56] Fisher M E, Ma S K and Nickel G G 1972 Critical exponent for long-range interactions *Phys. Rev. Lett.* **29** 917–20

[57] Huang K 1987 *Statistical Mechanics* 2nd edn (New York: Wiley)

[58] Blume M 1966 Monte Carlo simulation of polymer chain with ferromagnetic Ising interaction *Phys. Rev.* **141** 517–24

[59] da Silva R, Alves N A and Drugowich de Felício J R 2002 Universality and scaling of the two-dimencional Blume-Capel model in short-time dynamics *Phys. Rev.* E **66** 026130

[60] Kincaid J M and Cohen E G D 1975 Phase diagrams of liquid helium mixtures and metamagnets: experiment and mean field theory *Phys. Rep.* **22** 57–143

[61] Janssen H K and Oerding K 1994 Non-equilibrium relaxation at a tricritical point *J. Phys. A: Math. Gen.* **27** 715–23

[62] Xavier J C, Alcaraz F C, Penã Lara D and Plascak J A 1998 Critical behavior of the spin-3/2 Blume–Capel model in two dimensions *Phys. Rev.* B **57** 11575–81

[63] Friedan D, Qiu Z and Shenker S 1984 Conformal invariance, unitarity, and critical exponents in two dimensions *Phys. Rev. Lett.* **52** 1575–8

[64] Albano E V and Binder K in preparation

[65] Stryjewski E and Giordano N 1977 Metamagnetism *Adv. Phys.* **26** 487–650

[66] Santos M and Figueiredo W 2000 Short-time dynamic of a metamagnetic model *Phys. Rev.* E **62** 1799–804

[67] Plascak J A and Landau D P 2003 Universality and double critical end point *Phys. Rev.* E **67** 015103

[68] Grandi B C S and Figueiredo W 2004 Short-time dynamics for the spin-3/2 Blume–Capel model *Phys. Rev.* E **70** 056109

[69] Hao L and Yang Z R 1987 Lacunarity and universality *J. Phys. A: Math. Gen.* **20** 1627–31

[70] Monceau P and Hsiao P 2004 Direct evidence for weak universality on fractal structures *Physica* A **331** 1–9

[71] Gefen Y, Mandelbrot B B and Aharony A 1980 Critical phenomena on fractal lattices *Phys. Rev. Lett.* **45** 855–8

[72] Gefen Y, Aharony A and Mandelbrot B 1984 Phase transitions on fractals. III. Infinitely ramified lattices *J. Phys. A: Math. Gen.* **17** 1277–90

[73] Monceau P and Hsiao P 2002 Anomalous dimension exponents on fractal structures for the Ising and three-state Potts model *Phys. Lett.* A **300** 687–90

[74] Sornette D 1998 Discrete-scale invariance and complex dimensions *Phys. Rep.* **297** 239–70

[75] Bab M A, Fabricius G and Albano E V 2008 On the occurrence of oscillatory modulations in the power law behavior of dynamic and kinetic processes in fractals *Europhys. Lett.* **81** 10003

[76] da Silva L F, Fulco U L and Nobre F D 2009 The two-dimensional site-diluted Ising model: a short-time-dynamics approach *J. Phys.: Condens. Matter* **21** 346005

[77] Martins P H L and Plascak J A 2007 Universality class of the two-dimensional site-diluted Ising model *Phys. Rev.* E **76** 012102

[78] Prudnicov P V, Prudnicov V V, Krinitsyn A S, Vakilov A N and Pospelov E A 2010 Short-time dynamics and critical behavior of the three-dimensional site-diluted Ising model *Phys. Rev.* E **81** 011130

[79] Luo H J, Schülke L and Zheng B 2001 Short-time critical dynamics of the two dimensional random-bond Ising model *Phys. Rev.* E **64** 036123

[80] Yin J Q, Zheng B and Trimper S 2004 Critical behavior of the two-dimensional random-bond Potts model: A short-time dynammic approach *Phys. Rev.* E **70** 056134

[81] Kim J-K 1996 Weak universality in the two-dimensional randomly disordered three-state potts ferromagnet *Phys. Rev.* B **53** 3388–91

[82] Ying H-P and Harada K 2000 Short-time dynamics and magnetic critical behavior of the two-dimensional random-bond potts model *Phys. Rev.* E **62** 174–8

[83] Yin J Q, Zheng B and Trimper S 2005 Dynamics monte carlo simulations of the three-dimensional random-bond potts model *Phys. Rev.* E **72** 036122

[84] Yin J Q, Zheng B, Prudnikov V V and Trimper S 2005 Short-time dynamics and critical behavior of

three-dimensional bond-diluted Potts model *Eur. Phys. J.* B **49** 195
[85] Lee H K and Okabe Y 2005 Reweighting for nonequilibrium markov processes using sequential importance sampling methods *Phys. Rev.* E **71** 015102
[86] Chatelain C, Berche B, Janke W and Berche P E 2001 Softening of first-order transition in three-dimensions by quenched disorder *Phys. Rev.* E **64** 036120
[87] Chatelain C, Berche B, Janke W and Berche P-E 2005 Monte Carlo study of phase transitions in the bond-diluted 3D 4-state Potts model *Nucl. Phys.* B **719** 275–311
[88] Zheng G P and Mo Li 2002 Effect of disorder on critical short-time dynamics *Phys. Rev.* E **65** 036130
[89] McCoy B M and Wu T T 1968 Theory of a two-dimensional Ising model with random impurities: I. Thermodynamics *Phys. Rev.* **176** 631–43
[90] Parisi G, Ricci-Tersenghi F and Ruiz-Lorenzo J J 1999 Universality in the off-equilibrium critical dynamics of the three-dimensional diluted Ising model *Phys. Rev.* E **60** 5198–201
[91] Ma S K 1976 *Modern Theory of Critical Phenomena* (Reading, MA: Benjamin)
[92] Binder K 1983 Critical behaviour at surfaces *Phase Transitions and Critical Phenomena* vol 8 ed C Domb and J L Lebowitz (London: Academic)
[93] Diehl H W 1986 Field-theoretical approach to critical behaviour at surfaces *Phase Transitions and Critical Phenomena* vol 10 ed C Domb and J L Lebowitz (London: Academic)
[94] Pleimling M 2004 Critical phenomena at perfect and non-perfect surfaces *J. Phys. A: Math. Gen.* **37** R79
[95] Dietrich S and Diehl H W 1983 The effects of surfaces on dynamic critical behavior *Z. Phys.* B **51** 343–54
[96] Diehl H W and Janssen H K 1992 Boundary conditions for the field theory of dynamic critical behavior in semi-infinite systems with conserved order parameter *Phys. Rev.* A **45** 7145–55
[97] Diehl H W 1994 Universality classes for the dynamic surface critical behavior of systems with relaxational dynamics *Phys. Rev.* B **49** 2846–60
[98] Wichmann F and Diehl H W 1995 Dynamic surface critical behavior of systems with conserved bulk order parameter: detailed RG analysis of the semi-infinite extensions of model B with and without nonconservative surface terms *Z. Phys.* B **97** 251–67
[99] Ritschel U and Czerner P 1995 Universal short-time behavior in critical dynamics near surfaces *Phys. Rev. Lett.* **75** 3882–5
[100] Majumdar S N and Sengupta A M 1996 Nonequilibrium dynamics following a quench to the critical point in a semi-infinite system *Phys. Rev. Lett.* **76** 2394–7
[101] Pleimling M and Iglói F 2004 Nonequilibrium critical dynamics at surfaces: cluster dissolution and nonalgebraic correlations *Phys. Rev. Lett.* **92** 145701
[102] Pleimling M and Iglói F 2005 Nonequilibrium critical dynamics in inhomogeneous systems *Phys. Rev.* B **71** 094424
[103] Zhou N J and Zheng B 2007 Non-equilibrium critical dynamics with domain interface *Europhys. Lett.* **78** 56001
[104] Zhou N J and Zheng B 2008 Nonequilibrium critical dynamics with domain wall and surface *Phys. Rev.* E **77** 051104
[105] Lin S Z and Zheng B 2008 Short-time critical dynamics at perfect and imperfect surfaces *Phys. Rev.* E **78** 011127
[106] Pleimling M 2004 Aging phenomena in critical semi-infinite systems *Phys. Rev.* B **70** 104401
[107] Gambassi A and Dietrich S 2006 Critical dynamics in thin films *J. Stat. Phys.* **123** 929–1005
[108] Diehl H W and Chamati H 2009 Dynamic critical behavior of model *a* in films: zero-mode boundary conditions and expansion near four dimensions *Phys. Rev.* B **79** 104301
[109] Ruge C, Dunkelmann A and Wagner F 1992 New method for determination of critical parameters *Phys. Rev. Lett.* **69** 2465–7
[110] Simões C S and Drugowich de Felicio J R 1998 Nonuniversality in short-time critical dynamics *J. Phys. A: Math. Gen.* **31** 7265–72
[111] Fan C and Wu F Y 1969 Ising model with second-neighbor interaction: I. Some exact results and an approximate solution *Phys. Rev.* **179** 560–9
[112] Lima A R, de Oliveira P M C and Penna T J P 2000 Broad histogram method for multiparametric hamiltonians *Solid. State Commun.* **114** 447–52
[113] Alves N and Drugowich de Felicio J R 2003 Short-time dynamic exponents of an Ising model with competing interactions *Mod. Phys. Lett.* B **17** 209–18
[114] Calabrese P, Parruccini P, Pelissetto A and Vicari E 2004 Critical behavior of o(2)xo(n) symmetric models *Phys. Rev.* B **70** 174439
[115] Pelissetto A, Rossi P and Vicari E 2001 Critical behavior of frustrated spin models with noncollinear order *Phys. Rev.* B **63** 140414R
[116] Delamotte B, Mouhanna D and Tissier M 2004 Nonperturbative renormalization-group approach to frustrated magnets *Phys. Rev.* B **69** 134413
[117] Delamotte B, Mouhanna D and Tissier M 2004 Frustrated magnets in three dimensions: a nonperturbative approach *J. Phys.: Condens. Matter.* **16** S883–9
[118] Kawamura H 1992 Frustrated magnets in three dimensions: a nonperturbative approach *J. Phys. Soc. Japan.* **61** 1299–325
[119] Itakura M 2003 Monte Carlo renormalization group study of the Heisenberg and XY antiferromagnets on the stacked triangular lattice and the chiral ϕ^4 model *J. Phys. Soc. Japan.* **72** 74–82
[120] Bekhechi S, Southern B W, Peles A and Mouhanna D 2006 Short-time dynamics of a family of XY noncollinear magnets *Phys. Rev.* E **74** 016109
[121] Kosterlitz J M and Thouless D J 1973 Ordering, metastability and phase transitions in two-dimensional systems *J. Phys. C: Solid State Phys.* **6** 1181–203
[122] Kosterlitz J M 1974 The critical properties of the two-dimensional XY model *J. Phys. C: Solid State Phys.* **7** 1046–60
[123] Scheinine A L 1989 Fourier-accelerated Langevin simulation of the frustrated XY model *Phys. Rev.* B **39** 9368–76
[124] Gupta R and Baillie C F 1992 Critical behavior of the two-dimensional XY model *Phys. Rev.* B **45** 2883–98
[125] Olsson P 1995 Two phase transitions in the fully frustrated XY model *Phys. Rev. Lett.* **75** 2758–61
[126] Lee S and Lee K C 1994 Phase transitions in the fully frustrated XY model studied with use of the microcanonical Monte Carlo technique *Phys. Rev.* B **49** 15184–9
[127] José J V, Kadanoff L P, Kirkpatrick S and Nelson D R 1977 Renormalization, vortices, and symmetry-breaking perturbations in the two-dimensional planar model *Phys. Rev.* B **16** 1217–41
[128] Challa M S S and Landau D P 1986 Critical behavior of the six-state clock model in two dimensions *Phys. Rev.* B **33** 437–43
[129] Okano K, Schülke L, Yamagishi K and Zheng B 1997 Monte Carlo simulation of the short-time behaviour of the dynamic XY-model *J. Phys. A: Math. Gen.* **30** 4527–35
[130] Czerner P and Ritschel U 1996 Universal short-time dynamics in the kosterlitz–thouless phase *Phys. Rev.* E **53** 3333–41

[131] Luo H J, Schülke L and Zheng B 1998 Dynamic approach to the fully frustrated XY model *Phys. Rev. Lett.* **81** 180–3

[132] Luo H J and Zheng B 1997 Critical relaxation and critical exponents *Mod. Phys. Lett.* B **11** 615–23

[133] Ramirez-Santiago G and José J V 1994 Critical exponents of the fully frustrated two-dimensional XY model *Phys. Rev.* B **49** 9567–82

[134] Rutenberg A D and Bray A J 1995 Phase ordering of two-dimensional XY systems below the Kosterlitz–Thouless transition temperature *Phys. Rev.* E **51** R1641–4

[135] Mézard M, Parisi G and Virasoro M 1987 *Spin Glass Theory and Beyond* (Singapore: World Scientific)

[136] Bhatt R N and Young A P 1988 Numerical studies of Ising spin glasses in two, three, and four dimensions *Phys. Rev.* B **37** 5606–14

[137] Rieger H 1993 Nonequilibrium dynamics and aging in the three-dimensional Ising spin-glass model *J. Phys. A: Math. Gen.* **26** L615

[138] Ogielski A T 1985 Dynamics of three-dimensional Ising spin glasses in thermal equilibrium *Phys. Rev.* B **32** 7384–98

[139] Blundell R E, Humanyun K and Bray A J 1992 Dynamic exponent of the 3d Ising spin glass *J. Phys. A: Math. Gen.* **25** L733

[140] Bhatt R N and Young A P 1992 A new method for studying the dynamics of spin glasses *Euro Phys. Lett.* **20** 59

[141] Ozeki Y and Ito N 2001 Nonequilibrium relaxation study of Ising spin glass models *Phys. Rev.* B **64** 024416

[142] Hansmann U H E and Okamoto Y 1999 Finite-size scaling of helix–coil transitions in poly-alanine studied by multicanonical simulations *J. Chem. Phys.* **110** 1267–76

[143] Alves N A and Hansmann U H E 2000 Partition function zeros and finite size scaling of helix–coil transitions in a polypeptide *Phys. Rev. Lett.* **84** 1836–9

[144] Arashiro E, Drugowich de Felício J R and Hansmann U H E 2006 Short-time dynamics of the helix–coil transition in polypeptides *Phys. Rev.* E **73** 040902

[145] Arashiro E, Drugowich de Felício J R and Hansmann U H E 2007 Short-time dynamics of polypeptides *J. Chem. Phys.* **126** 045107

[146] Rubio Puzzo M L and Albano E V 2008 The damage spreading method in Monte Carlo simulations: a brief overview and applications to confined magnetic materials *Commun. Comput. Phys.* **4** 207–30

[147] Herrmann H J 1992 *The Monte Carlo Method in Condensed Matter Physics* ed K Binder (Berlin: Springer)

[148] Herrmann H J 1990 Damage spreading *Physica* A **168** 516–28

[149] Grassberger P 1989 Directed percolation in 2 + 1 dimensions *J. Phys. A: Math. Gen.* **22** 3673–9

[150] Grassberger P 1995 Damage spreading in the Ising model with glauber dynamics *J. Phys. A: Math. Gen.* **28** L67–72

[151] Grassberger P 1995 Are damage spreading transitions generically in the universality class of directed percolation? *J. Stat. Phys.* **79** 13–23

[152] Broadbent S R and Hammersley J M 1957 Percolation processes *Math. Proc. Camb. Phil. Soc.* **53** 629–41

[153] Jensen I 1999 Low-density series expansions for directed percolation: I. A new efficient algorithm with applications to the square lattice *J. Phys. A: Math. Gen.* **32** 5233–49

[154] Voigt C A and Ziff R M 1997 Epidemic analysis of the second-order transition in the Ziff–Gulari–Barshad surface-reaction model *Phys. Rev.* E **56** R6241–4

[155] Hinrichsen H, Domany E and Stauffer D 1998 Damage spreading in a 2d Ising model with swendsenwang dynamics *J. Stat. Phys.* **91** 807–14

[156] Bagnoli F, Rechtman R and Ruffo S 1992 Damage spreading and lyapunov exponents in cellular automata *Phys. Lett.* A **172** 34–8

[157] Kauffman S A 1969 Metabolic stability and epigenesis in randomly constructed genetic nets *J. Theor. Biol.* **22** 437–67

[158] Kauffman S A 1984 Emergent properties in random complex automata *Physica* D **10** 145–56

[159] Albano E V 1994 Damage spreading in the Ziff–Gulari–Barshad model *Phys. Rev.* E **50** 1129–34

[160] Grassberger P 1995 Damage spreading and critical exponents for model a Ising dynamics *Physica* A **214** 547–59

[161] Rubio Puzzo M L and Albano E V 2010 Short-time critical dynamics of damage spreading in the two-dimensional Ising model *Phys. Rev.* E **81** 051116

[162] Montani F and Albano E V 1995 Dynamics of damage spreading in the two-dimensional Ising magnet at criticality *Phys. Lett.* A **202** 253–7

[163] Marro J and Dickman R 1999 *Nonequilibrium Phase Transitions and Critical Phenomena* (Cambridge: Cambridge University Press)

[164] Loscar E S and Albano E V 2003 Critical behaviour of irreversible reaction systems *Rep. Prog. Phys.* **66** 1343–82

[165] Ozeki Y, Kasono K, Ito N and Miyashita S 2003 Nonequilibrium relaxation analysis for first-order phase transitions *Physica* A **321** 271–9

[166] Zheng G 2002 Short-time dynamics of first-order phase transition in a disordered system *J. Phys. A: Math. Gen.* **35** 10549–61

[167] Schülke L and Zheng B 2000 Dynamic approach to weak first-order phase transitions *Phys. Rev.* E **62** 7482–5

[168] Saracco G P and Albano E V 2003 Critical and dynamical behavior of a driven diffusive lattice gas *J. Chem. Phys.* **118** 4157–63

[169] Albano E V 2001 Monte Carlo simulations of the short time dynamics of a first-order irreversible phase transition *Phys. Lett.* A **288** 73–8

[170] Loscar E S, Ferrero E E, Grigera T S and Cannas S A 2009 Nonequilibrium characterization of spinodal points using short time dynamics *J. Chem. Phys.* **131** 024120

[171] Binder K 2007 Double-well thermodynamic potentials and spinodal curves: How real are they? *Phil. Mag. Lett.* **87** 799–811

[172] Kihara T, Midzuno Y and Shizume T 1954 Statistics of two-dimensional lattices with many components *J. Phys. Soc. Japan* **9** 681–7

[173] Gulbahce N, Gould H and Klein W 2004 Zeros of the partition function and pseudospinodals in long-range Ising models *Phys. Rev.* E **69** 036119

[174] Herrmann D W, Klein W and Stauffer D 1982 Spinodals in a long-range interaction system *Phys. Rev. Lett.* **49** 1262–4

[175] Fernández L A, Ruiz-Lorenzo J J, Lombardo M P and Tarancón A 1992 Weak first order transitions. the two-dimensional potts model *Phys. Lett.* B **277** 485–90

[176] Rácz Z 2004 Nonequilibrum phase transitions *Slow Relaxations and Nonequilibrum Dynamics in Condensed Matter* (Les Hauches School) ed M Feigelman and J Kurchan (Berlin: Springer) arxiv.org/abs/cond-mat/0303156

[177] Haken H 1978 *Synergetics* (New York: Springer)

[178] Cross M C and Hohenberg P C 1993 Pattern formation outside of equilibrium *Rev. Mod. Phys.* **65** 851–1112

[179] Katz S, Lebowitz J L and Spohn H 1983 Phase transitions in stationary nonequilibrium states of model lattice systems *Phys. Rev.* B **28** 1655–8

[180] Schmittmann B and Zia R K P 1995 Scaling and renormalization in statistical physics *Statistical Mechanics of Driven Diffusive Systems* (London: Academic)

[181] Hurtado P I, Marro J, Garrido P L and Albano E V 2003 Kinetics of phase separation in the driven lattice gas: Self-similar pattern growth under anisotropic nonequilibrium conditions *Phys. Rev.* B **67** 014206

[182] Janssen H K and Schmittmann B 1986 Field theory of critical behaviour in driven diffusive systems *Z. Phys.* B **64** 503–14

[183] Leung K-T and Cardy J L 1986 Field theory of critical behavior in a driven diffusive system *J. Stat. Phys.* **44** 567–88

[184] Leung K-T and Cardy J L 1986 Field theory of critical behavior in a driven diffusive system *J. Stat. Phys.* **45** 1087 (erratum)

[185] Vallés J L and Marro J 1987 Nonequilibrium second-order phase transitions in stochastic lattice systems: a finite-size scaling analysis in two dimensions *J. Stat. Phys.* **49** 89

[186] Leung K-T 1991 Finite-size scaling of driven diffusive systems: Theory and Monte Carlo studies *Phys. Rev. Lett.* **66** 453–6

[187] Achahbar A and Marro J 1995 Phase transitions in a driven lattice gas in two planes *J. Stat. Phys.* **78** 1493

[188] Marro J, Achahbar A, Garrido P L and Alonso J J 1996 Phase transitions in driven lattice gases *Phys. Rev.* E **53** 6038

[189] de los Santos F, Garrido P L and Muñoz M A 2001 Entropic contributions in Langevin equations for anisotropic driven systems *Physica* A **61** 364

[190] Schmittmann B and Zia R K P 1991 Critical properties of a randomly driven diffusive system *Phys. Rev. Lett.* **66** 357–60

[191] Garrido P L, de los Santos F and Muñoz M A 1998 Langevin equation for driven diffusive systems *Phys. Rev.* E **57** 752–5

[192] Garrido P L, Muñoz M A and de los Santos F 2000 Universality classes of driven lattice gases *Phys. Rev.* E **61** R4683–6

[193] de los Santos F, Garrido P L and Mu noz M A 2001 Entropic contributions in Langevin equations for anisotropic driven systems *Physica* A **296** 364–74

[194] Achahbar A, Garrido P L, Marro J and Muñoz M A 2001 Is the particle current a relevant feature in driven lattice gases? *Phys. Rev. Lett.* **87** 195702

[195] Albano E V and Saracco G 2002 Dynamic behavior of anisotropic nonequilibrium driving lattice gases *Phys. Rev. Lett.* **88** 145701

[196] Albano E V and Saracco G 2004 Albano and Saracco reply *Phys. Rev. Lett.* **92** 029602

[197] Caracciolo S, Gambassi A, Gubinelli M and Pelissetto A 2004 Comment on ıdynamic behavior of anisotropic nonequilibrium driving lattice gases *Phys. Rev. Lett.* **92** 029601

[198] Couzin I D, Krause J, Franks N R and Levin S A 2005 Effective leadership and decision-making in animal groups on the move *Nature* **433** 513–16

[199] Chowdhury D, Nishinari K and Schadschneider A 2004 Self-organized patterns and traffic flow in colonies of organisms: from bacteria and social insects to vertebrates *Phase Transit.* **77** 601–24

[200] Feder T 2007 Statistical physics is for the birds *Phys. Today* **60** 28–30

[201] Becco Ch, Vandewalle N, Delcourt J and Poncin P 2006 Experimental evidences of a structural and dynamical transition in fish school *Physica* A **367** 487–93

[202] Bonner J T 1998 A way of following individual cells in the migrating slugs of dictyostelium discoideum *Proc. Natl Acad. Sci.* **95** 9355–9

[203] Rappel W J, Nicol A, Sarkissian A, Levine H and Loomis W F 1999 Self-organized vortex state in two-dimensional dictyostelium dynamics *Phys. Rev. Lett.* **83** 1247–50

[204] Ben-Jacob E, Cohen I, Czirók A, Vicsek T and Gutnick D L 1997 Chemomodulation of cellular movement, collective formation of vortices by swarming bacteria, and colonial development *Physica* A **238** 181–97

[205] Vicsek T, Czirók A, Ben-Jacob E, Cohen I and Shochet O 1995 Novel type of phase transition in a system of self-driven particles *Phys. Rev. Lett.* **75** 1226–9

[206] Baglietto G and Albano E V 2008 Finite-size scaling analysis and dynamic study of the critical behavior of a model for the collective displacement of self-driven individuals *Phys. Rev.* E **78** 021125

[207] Bray A J, Briant A J and Jervis D K 2000 Breakdown of scaling in the nonequilibrium critical dynamics of the two-dimensional XY model *Phys. Rev. Lett.* **84** 1503–6

[208] Wood K, Van den Broeck C, Kawai R and Lindenberg K 2007 Synchrony and critical behavior: equilibrium universality in nonequilibrium stochastic oscillators *AIP Conf. Proc.* **913** 49–55

[209] Marro J and Dickman R 1999 *Nonequilibrium Phase Transitions in Lattice Models* (Cambridge: Cambridge Univerity Press)

[210] Hinrichsen H 2000 Non-equilibrium critical phenomena and phase transitions into absorbing states *Adv. Phys.* **49** 815–958

[211] Hinrichsen H 2006 Fundamental problems in statistical physics *Proc. 11th Int. Summerschool on 'Fundamental Problems in Statistical Physics'* (Leuven, Belgium) *Physica* A **369** 1–28

[212] Ódor G 2004 Universality classes in nonequilibrium lattice systems *Rev. Mod. Phys.* **76** 663–724

[213] Bak P, Tang C and Wiesenfeld K 1987 Self-organized criticality: an explanation of the 1/f noise *Phys. Rev. Lett.* **59** 381–4

[214] Bak P, Tang C and Wiesenfeld K 1988 Self-organized criticality *Phys. Rev.* A **38** 364–74

[215] Bak P 1996 *How Nature Works: the Science of Self-Organized Criticality* (New York: Copernicus/Springer)

[216] Jensen H J 1998 *Self-Organized Criticality* (Cambridge: Cambridge University Press)

[217] Laneri K, Rozenfeld A F and Albano E V 2005 Dynamic critical approach to self-organized criticality *Phys. Rev.* E **72** 065105

[218] Bak P and Sneppen K 1993 Punctuated equilibrium and criticality in a simple model of evolution *Phys. Rev. Lett.* **71** 4083–6

[219] Flyvbjerg H, Sneppen K and Bak P 1993 Mean field theory for a simple model of evolution *Phys. Rev. Lett.* **71** 4087–90

[220] Sneppen K, Bak P, Flyvbjerg H and Jensen M H 1995 Evolution as a self-organized critical phenomenon *Proc. Natl Acad. Sci. USA* **92** 5209–13

[221] Bak P and Paczuski M 1995 Complexity, contingency, and criticality *Proc. Natl Acad. Sci. USA* **92** 6689–96

[222] Paczuski M, Maslov S and Bak P 1996 Avalanche dynamics in evolution, growth, and depinning models *Phys. Rev.* E **53** 414–43

[223] Conway J H, Belekamp E R and Guy R K 1982 *Winning Ways for your Mathematical Plays* vol 2 (New York: Academic)

[224] Rozenfeld A, Laneri K and Albano E V 2007 Critical dynamic approach to stationary states in complex systems *Eur. Phys. J. Spec. Top.* **143** 3–8